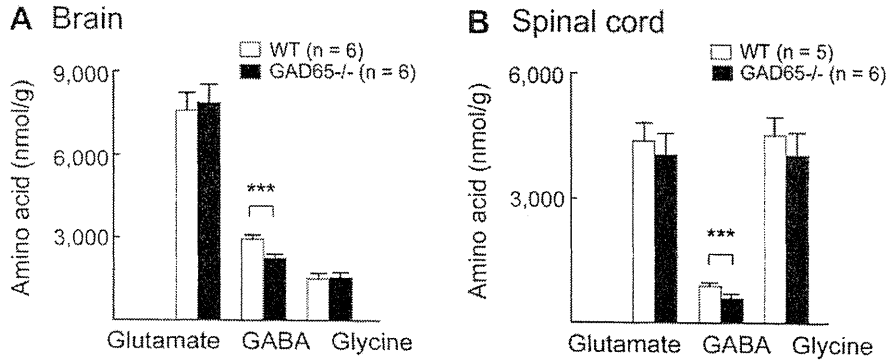

Fig. 1. GABA contents of GAD65−/− mice are reduced in the brain (A) and the spinal cord (B). Neurotransmitter contents were analyzed by high-performance liquid chromatography (HPLC). (A) In the whole brain, GABA contents were significantly reduced in GABA65−/− mice ($n = 6$, $P < 0.001$, t-test) compared with those of WT mice ($n = 6$). Data bars show mean ± SD. (B) In the spinal cord, GABA contents were also significantly reduced in GAD65−/− mice ($n = 6$, $P < 0.001$, t-test). Note that glutamate and glycine contents were unaffected by GAD65 gene knockout in the brain and the spinal cord. Data bars show mean ± SD.

frontal cortex of mice. The effects of PIC on the holding current were examined in the absence of the anesthetic. Although PIC (50 μM, 5 min) produced an inward shift in all groups, the amplitude of tonic current was slightly but significantly reduced in GAD65−/− mice (13.3 ± 5.5 pA in GAD65−/− slices, $n = 12$; 24.4 ± 6.5 pA in WT slices, $n = 11$, $P < 0.001$, Fig. 2B). On the other hand, the tonic conductance was significantly increased in WT mice treated with a GAT-1 inhibitor NO-711 (3 mg/kg, ip) (34.5 ± 7.8 pA, $n = 12$, $P < 0.01$ vs. WT slices, Fig. 2B). These data provide indirect evidence that ambient GABA levels in the frontal cortex are altered by genetic and pharmacological manipulations used in the present study.

3.3. Behavioral responses to sevoflurane are unchanged in GAD65−/− mice

We next examined whether the anesthetic sensitivity to sevoflurane is altered by GAD65 gene knockout. The LORR assay was performed to examine the anesthetic sensitivity of mice to sevoflurane. Mice were judged to have lost this reflex when unable to right itself within 10 s. The dose–response curves for the ED_{50} determination for LORR are presented in Fig. 3A. The calculated ED_{50} values for LORR were 1.24% in WT mice ($n = 14$) and 1.26% in GAD65−/− mice ($n = 14$). Thus, GAD65 gene knockout did not affect anesthetic sensitivity to sevoflurane. LTWR was used as a surrogate measure for immobilization (Quasha et al., 1980). Sevoflurane concentration was increased and the ED_{50} value for LTWR was determined. The calculated ED_{50} values for LTWR were 2.07% in WT mice ($n = 21$) and 2.04% in GAD65−/− mice ($n = 21$). These data suggest that hypnotic and immobilizing actions of sevoflurane are unaffected by GAD65 gene knockout and resulting reduction in GABA content (Fig. 1).

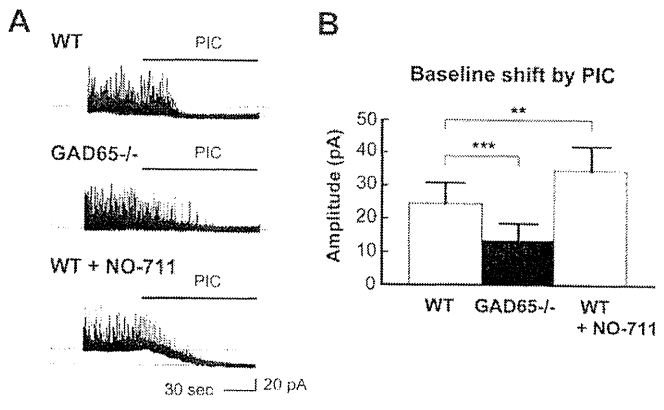

Fig. 2. The effects of genetic and pharmacological manipulations on the amplitude of tonic inhibition in cortical layer V neurons. Neurons were voltage-clamped at 0 mV using Cs_2SO_4-based internal solutions. (A) Representative traces of mIPSCs from WT slices (top), GAD65−/− slices (middle), and WT with NO-711 slices (bottom). These mIPSCs were completely blocked after application of picrotoxin (PIC, 50 μM) in all groups. (B) Baseline shift produced by PIC (50 μM) was significantly smaller in cortical neurons of GAD65−/− slices (***$P < 0.001$ vs. WT), and larger in cortical neurons of WT with NO-711 slices (**$P < 0.01$ vs. WT). Data bars show mean ± SD.

3.4. Behavioral response to propofol and midazolam are diminished in GAD65−/− mice

We then compared anesthetic sensitivity to propofol and midazolam, a positive allosteric modulator of $GABA_A$ receptors. The latency to LORR produced by propofol (125 mg/kg, ip) was significantly prolonged in GAD65−/− mice (188.9 ± 23.6 s, $n = 10$, $P < 0.01$,) than that of WT mice (150.0 ± 27.5 s, $n = 10$). The duration of LORR produced by propofol (125 mg/kg, ip) was significantly reduced in GAD65−/− mice (1568.0 ± 689.0 s, $n = 10$, $P < 0.05$) than that of WT mice (2263.0 ± 533.6 s, $n = 10$, Fig. 3B *left*). Similarly, the duration of LTWR produced by propofol (125 mg/kg, ip) was significantly reduced in GAD65−/− mice ($n = 8$, $P < 0.01$, Fig. 3B *right*). As shown in Fig. 3C, the duration of LORR produced by midazolam (50 mg/kg, ip) was significantly reduced in GAD65−/− mice (2498.4 ± 1351.0 s, $n = 9$, $P < 0.05$) than that of WT mice (3564.0 ± 854.0 s, $n = 21$) without affecting the latency to LORR ($P = 0.60$ between genotypes). In addition, the duration of LTWR produced by midazolam (50 mg/kg, ip) was significantly reduced in GAD65−/− mice ($n = 8$ each, $P < 0.05$).

3.5. Behavioral responses to sevoflurane are unchanged by GABA transporter 1 inhibition

We then tested whether the selective GAT-1 inhibitor, NO-711, would affect LORR produced by sevoflurane, propofol and midazolam. Because enhanced GABA concentration by NO-711 may produce hypnotic actions in the absence of the anesthetics, we first confirmed that NO-711 at low doses (1 or 3 mg/kg, ip) had no effect on righting reflex in both genotypes. Righting reflex was slightly impaired at 6 mg/kg (ip) and severely impaired at high doses (>10 mg/kg). These data suggest that NO-711 alone can induce hypnosis in a dose-dependent manner by enhancing tonic inhibitions.

NO-711 (3 mg/kg, ip) did not affect dose–response relationship of LORR produced by sevoflurane (Fig. 4A). The calculated ED_{50}

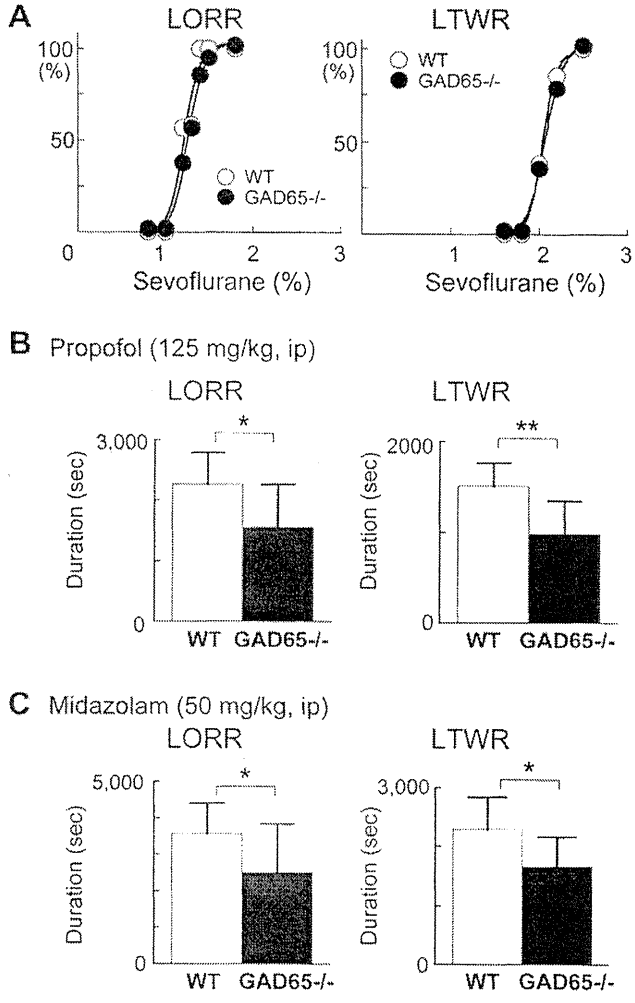

Fig. 3. The effects of reduced GABA contents by GAD65 gene knockout on behavioral responses to sevoflurane, propofol, and midazolam. (A) Dose–response curves for the determination of the ED_{50} value for loss of righting reflex (left) and for loss of tail-pinch withdrawal response (right) produced by sevoflurane. Data presented are the fraction of mice that did not respond, i.e., failed to right themselves on the LORR or failed to move in response to the tail clamp vs. sevoflurane concentration. The fitted curves were generated using a weighted sum of least-squares method (Kaleida-Graph version 3.5, Reading, PA) to a Hill equation: LORR (%) = $[drug]^{nH}/([drug]^{nH} + [ED_{50}]^{nH})$; where LORR (%) is a percentage of LORR, [drug] is the anesthetic concentration, and nH is the Hill coefficient. EC_{50} did not differ between genotypes for either assay. (B) The duration of LORR and LTWR were compared between WT mice and GAD65−/− mice. A significant reduction in the duration of LORR (*$P < 0.05$ between genotypes, $n = 10$) and LTWR (**$P < 0.01$) was observed in GAD65−/− mice. (C) A significant reduction in the duration of LORR and LTWR was observed in GAD65−/− mice (*$P < 0.05$ between genotypes, $n = 9$). Data bars show mean ± SD.

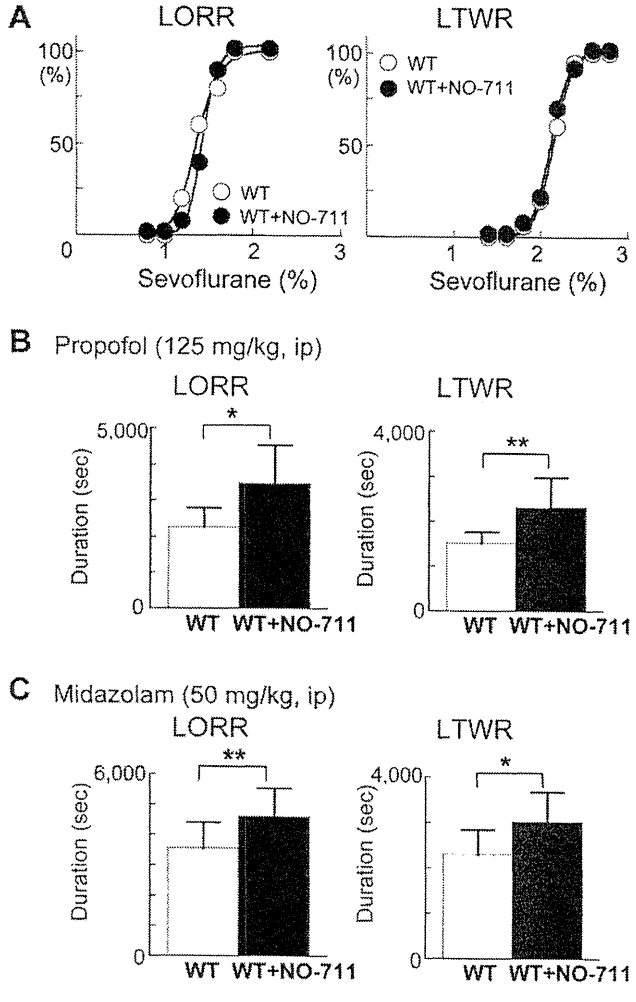

Fig. 4. The effects of increased GABA contents by NO-711 on behavioral responses to sevoflurane, propofol and midazolam. (A) Pre-injection of NO-711 (3 mg/kg, ip) had little effect on the dose–response relationship of LORR (left) and LTWR (right) produced by sevoflurane. (B) NO-711 (3 mg/kg, ip) significantly increased the duration of LORR ($n = 8$, *$P < 0.05$) and LTWR (**$P < 0.01$) produced by propofol (125 mg/kg, ip). (C) The effects of NO-711 (3 mg/kg, ip) on the duration of LORR and LTWR produced by midazolam (50 mg/kg, ip). NO-711 increased the duration of LORR ($n = 7$, **$P < 0.01$) and LTWR (*$P < 0.05$). Data bars show mean ± SD.

values for LORR were 1.28% in WT mice ($n = 10$) and 1.36% in GAD65−/− mice ($n = 10$). In LTWR assays, NO-711 (3.0 mg/kg, ip) had no effect on immobilizing actions produced by sevoflurane. The calculated ED_{50} values for LTWR were 2.15% in WT mice ($n = 13$) and 2.12% in WT mice with NO-711 (3 mg/kg, ip) ($n = 13$).

3.6. Behavioral responses to propofol and midazolam are enhanced by GAT-1 inhibition

NO-711 (3 mg/kg, ip) significantly increased the duration of LORR produced by propofol (125 mg/kg, ip) from 2263.0 ± 533.6 s ($n = 10$) to 3471.7 ± 1076.1 s ($n = 8$, $P < 0.05$, Fig. 4B) in WT mice without affecting the latency to LORR ($n = 8$, $P = 0.66$). NO-711 (3 mg/kg, ip) also increased the duration of LTWR ($P < 0.01$) produced by propofol (125 mg/kg, ip, Fig. 4B *right*). NO-711 (3.0 mg/kg) increased the duration of LORR produced by midazolam (50 mg/kg, ip) from 3564.0 ± 854.0 s to 4601.0 ± 951.0 s ($n = 7$, $P < 0.01$, Fig. 3C *left*) without affecting the latency to LORR ($n = 7$, $P = 0.89$). NO-711 (3 mg/kg, ip) increased the duration of LTWR ($n = 7$, $P < 0.05$) produced by midazolam (50 mg/kg, ip, Fig. 4C *right*).

3.7. Sevoflurane-induced enhancement of phasic and tonic inhibition

Intravenous anesthetic such as propofol and thiopental strongly enhance both phasic and tonic inhibition (Bai et al., 2001; Bieda and MacIver, 2004; Bieda et al., 2009). However, little is known about the effects of sevoflurane on phasic and tonic components of GABAergic inhibition. Although basal inhibitory synaptic transmission was normal in GAD65−/− mice (Kubo et al., 2009a; Tian et al., 1999) and WT mice with NO-711, sevoflurane enhanced GABAergic inhibition in cortical pyramidal neurons. Sevoflurane (0.23 mM) significantly increased the frequency of mIPSCs in WT

mice (180.1% of WT control, $n = 8$, $P < 0.001$), GAD65−/− mice (168.9% of GAD65−/− mice control, $n = 8$, $P < 0.001$), and WT with NO-711 (ip) (195.0% of NO-711 control, $n = 8$, $P < 0.001$). There was no group difference in the frequency in the presence of sevoflurane (0.23 mM, ANOVA). Sevoflurane (0.23 mM) also increased the decay time of mIPSCs in WT mice (241.1% of WT control, $n = 8$, $P < 0.001$), GAD65−/− mice (232.9% of GAD65−/− mice control, $n = 8$, $P < 0.001$), and WT with NO-711 (ip) (267.0% of NO-711 control, $n = 8$, $P < 0.001$). There was no group difference in the decay time in the absence or presence of sevoflurane (ANOVA). In addition, sevoflurane (0.23 M) produced a relatively small but significant baseline shift in I_{hold} in all groups (Fig. 5A). The amplitudes of baseline shift produced by sevoflurane were 13.1 ± 5.0 pA in WT mice ($n = 8$, $P < 0.001$ vs. control), 11.2 ± 3.9 pA in GAD65−/− mice ($n = 8$, $P < 0.001$ vs. control), and 14.9 ± 5.9 pA in WT mice with NO-711 (ip) ($n = 8$, $P < 0.001$ vs. control, Fig. 5B). These sevoflurane effects were reversible after washout of the anesthetic.

A specific $GABA_A$ receptor antagonist, SR95531 (1 μM), selectively blocks only synaptic $GABA_A$ receptors that generate IPSCs (Yamada et al., 2007), while PIC blocks both synaptic and extrasynaptic tonic conductances (Bieda and MacIver, 2004). SR95531 does not affect GABA-transaminase or GAD activities. To examine the relative contributions of synaptic components in GABAergic inhibition, we tested the effects of SR95531 (1 μM) on mIPSCs in the presence of sevoflurane (0.23 mM). SR95531 (1 μM, 5 min) abolished mIPSCs in all groups but had little effect on baseline holding current (WT slices, $n = 5$; GAD65−/− slices, $n = 4$; WT slices with NO-711, $n = 5$). Prolonged application (20 min) produced a small baseline shift in I_{hold} in all group, these changes did not reach statistical significance because of their variability.

3.8. Sevoflurane-induced depression of pyramidal neuron excitability

Whole cell recordings were obtained from visually identified layer V pyramidal neurons located within the medial PFC. Resting membrane potentials were −71.3 ± 2.6 mV ($n = 15$) in WT slices, −70.6 ± 3.5 mV ($n = 14$) in GAD65−/− slices, and 71.7 ± 3.9 mV ($n = 15$) in WT slices with NO-771. The majorities of neurons were typically silent at rest and were held for periods for >15 min. Although bath application of sevoflurane (0.23 mM, 20 min) produced a small hyperpolarization in all groups, but these effects did not reach statistical significance because of cell to cell variability. Sevoflurane (0.41 mM, 20 min) significantly hyperpolarized the neuron (−5.3 ± 2.5 mV in WT slices, $n = 8$; −6.3 ± 3.6 mV in GAD65−/− slices, $n = 8$; −7.3 ± 4.0 mV in WT slices with NO-711, $n = 8$).

In response to supra-threshold currents, some pyramidal neurons exhibited modest spike frequency accommodation, other neurons responded to current injection with relatively regular inter-spike intervals. Sevoflurane-induced neural depression was compared by measuring the number of APs to depolarizing current injection, as a measure of effects on intrinsic excitability. We focused on pyramidal neurons with relatively regular inter-spike intervals (Fig. 6A). In WT mice, sevoflurane (0.23 mM, 20 min) did not change action potential discharge responses to depolarizing

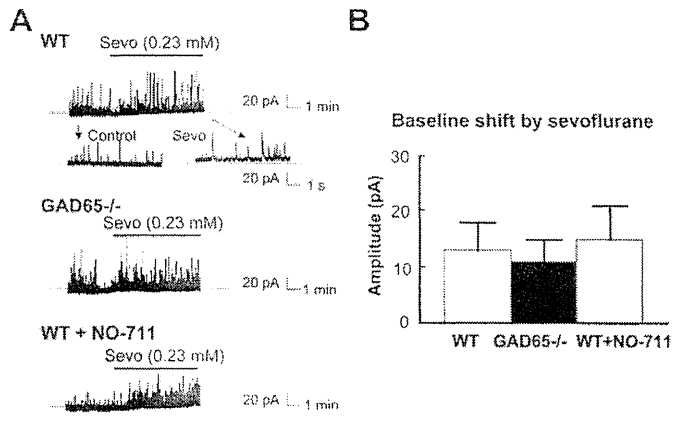

Fig. 5. The effects of sevoflurane (0.23 mM) on mIPSCs recorded from layer V pyramidal neurons n WT mice, GAD65−/− mice and WT mice with NO-711 injection. (A) Sample traces show spontaneous IPSCs recorded in normal ACSF solution in the presence of TTX (1 μM). Neurons were voltage-clamped at 0 mV using Cs_2SO_4-based internal solutions, and mIPSCs were recorded from WT mice (top), GAD65−/− mice (middle), and WT mice with NO-711 injection (bottom). Note that sevoflurane (0.23 mM, 20 min) increased the frequency and prolonged the decay phase, and also shifted the baseline. The effects of sevoflurane on the baseline currents reached plateau 5–10 min after sevoflurane application. (B) Sevoflurane (0.23 mM) slightly but significantly produced a baseline shift in all groups ($P < 0.05$ vs. control, $n = 8$). There was no significant difference among groups. Data bars show mean ± SD.

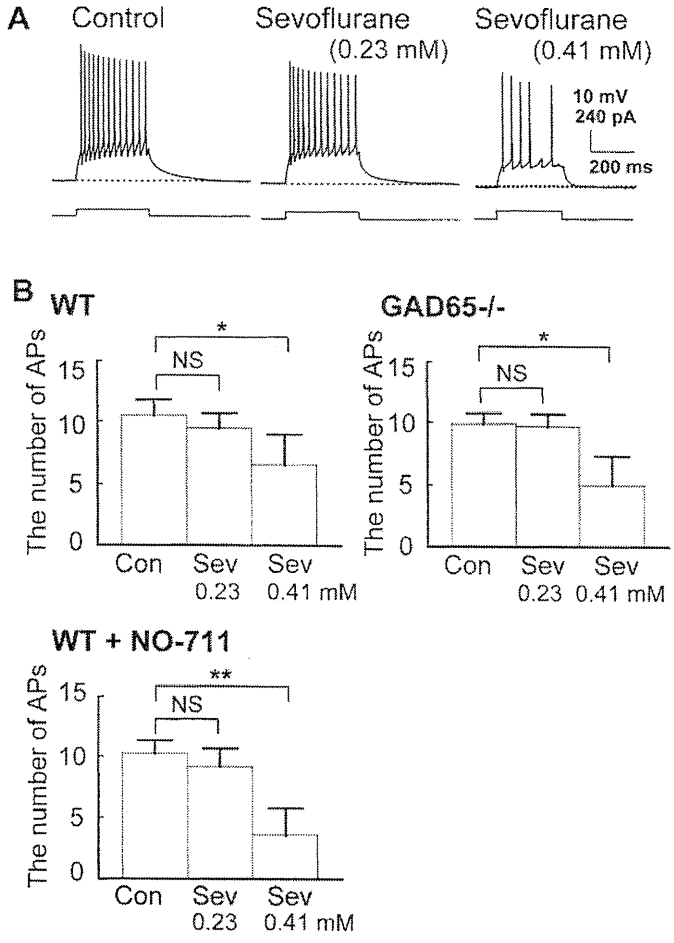

Fig. 6. The effects of sevoflurane on voltage responses to depolarizing current injection to pyramidal neurons with non-accommodating response. Recordings were made in whole cell current clamp using K-gluconate as the internal solution. (A) Representative examples of sevoflurane (0.23 mM) effects on AP discharge activity of cortical neurons in WT mice. The number of AP discharge induced by current injection (120 pA, 300 ms) was not altered by sevoflurane at clinically relevant concentration (0.23 mM), but inhibited by high concentration of sevoflurane (0.41 mM). (B) The effects of sevoflurane on AP discharge were compared among WT mice, GAD65−/− mice, and WT with NO-711 mice. NO-711 (3 mg/kg) were injected intraperitoneally 20 min prior to brain slice preparation. In WT mice, sevoflurane at 0.41 mM, but not 0.23 mM, inhibited the number of APs ($P < 0.05$ vs. control, $n = 8$, ANOVA). Similarly, sevoflurane at 0.23 mM had no effect on AP discharge activity ($n = 8$ for GAD65−/− mice and $n = 9$ for WT + NO-711 mice, ANOVA). Data are presented as mean ± SD.

current in pyramidal neurons. The number of APs was significantly depressed when sevoflurane (0.41 mM) was applied to the chamber (Fig. 6B). In WT mice, sevoflurane at 0.41 mM significantly depressed the number of APs from 10.5 ± 1.3 to 6.5 ± 2.4 ($n = 10$, $P < 0.05$ vs. control, ANOVA-Tukey). Similar results were observed in GAD65−/− mice and WT mice with NO-711 (ip). Although sevoflurane at 0.23 mM had no effect on neuronal excitability of pyramidal neurons in GAD65−/− mice ($n = 9$) and WT mice with NO-711 (ip) ($n = 9$), sevoflurane at 0.41 mM significantly depressed the number of APs in GAD65−/− mice ($n = 9$, $P < 0.05$ vs. control, ANOVA-Tukey) and in WT mice with NO-711 (ip) ($n = 9$, $P < 0.01$ vs. control, ANOVA–Tukey). The membrane input resistance in pyramidal neurons was very similar in all groups under control conditions. Superfusion of sevoflurane 0.41 mM, but not 0.23 mM, reversibly reduced input resistance to a similar degree in all groups (91.3 ± 3.4% of control in WT slices, $n = 5$; 93.3 ± 4.3% of control in GAD65−/− slices, $n = 5$; 89.8 ± 5.4% of control in WT slices with NO-711, $n = 5$).

In separate experiments, NO-711 was directly added to the ACSF solution that was bathing the slice in the recording chamber. The effects of NO-711 on sevoflurane-induced depression of pyramidal neuron excitability were basically similar to those observed with intraperitoneally injected NO-711 (3 mg/kg). In the presence of NO-711 (2 μM), sevoflurane (0.23 mM) had little effect on neuronal excitability of pyramidal neurons ($n = 6$), whereas sevoflurane (0.41 mM) significantly depressed the number of APs ($n = 5$, $P < 0.01$ vs. control, ANOVA–Tukey).

4. Discussion

GAD65−/− mice appeared to show normal sensitivity to sevoflurane despite a 20–30% reduction in GABAergic inhibitory tone, whereas they showed reduced sensitivity to propofol and midazolam. In contrast, enhanced GABA concentrations by NO-711 prolonged the duration of LORR and LTWR by propofol and midazolam, but not sevoflurane. Sevoflurane enhanced tonic inhibition of layer V cortical neurons; however, these effects were not strong enough to alter discharge properties of cortical neurons. These data show that genetic and pharmacological manipulations designed to alter ambient GABA concentrations differentially regulate hypnotic and immobilizing actions of general anesthetics.

4.1. Reduced ambient GABA concentrations in GAD−/− mice

GAD65−/− mice appeared to show partial reductions in GABA concentrations in the whole brain and whole spinal cord. However, HPLC data include synaptic vesicular, intracellular, and extracellular (ambient) GABA concentrations. Patch-clamp studies confirmed that the amplitude of tonic inhibition was significantly reduced in GAD65−/− mice and that this reduction was relevant to HPLC data. Given that the amplitude of tonic inhibition reflects the ambient GABA concentration (Semyanov et al., 2004), we conclude that ambient GABA concentrations are reduced in GAD65−/− mice, and that reduced ambient GABA concentrations are responsible for altered behavioral responses to propofol (Kubo et al., 2009a) and midazolam.

Although a compensatory mechanism involving the balance between inhibitory and glutamatergic excitatory neurotransmission might have been expected, glutamate and glycine levels were unchanged. As a result, the ratio of excitatory to inhibitory neurotransmitter levels actually increased in GAD65−/− mice. It has been reported that the survival rate of GAD65−/− mice was thus significantly reduced, largely due to spontaneous seizures; only 2–3% of WT mice died before postnatal 25 weeks, whereas 25% of GAD65−/− mice died during the same period (Stork et al., 2000). To minimize the possibility of a generalized increase in CNS excitability and behavioral abnormality during experiments, 12–16-week old mice were used in our study. In fact, we have previously confirmed that excitatory synaptic transmission in hippocampal slices was normal in GAD65−/− mice, and that the survival rate was almost similar between genotypes at this stage (Kubo et al., 2009a).

4.2. Reduced sensitivity to propofol and midazolam, but not sevoflurane, in GAD65−/− mice

Our data are consistent with previous reports showing that GAD65−/− mice had reduced sensitivity to pentobarbital, which is known to potentiate GABAergic inhibition (Kash et al., 1999). Although the molecular and cellular factors underlying differences in anesthetic sensitivity are currently unknown, one possibility is that sevoflurane may have multiple molecular targets contributing to *in vivo* hypnotic actions (Mascia et al., 1996; Sirois et al., 2000; Sonner et al., 2003; Chen et al., 2005; Wu et al., 2004). If so, the present data lead us to believe that relatively small changes in ambient GABA concentrations are insufficient to alter behavioral responses to sevoflurane. To support this notion, sevoflurane has been shown to depress excitatory synapses in synaptosomes (Moe et al., 2003), the brainstem (Stucke et al., 2005), and the hippocampus (Ishizeki et al., 2008), whereas propofol has little effect on excitatory synapses in cortical neurons (Kitamura et al., 2003), the hippocampus (Kubo et al., 2009a), and the spinal cord (Takazawa et al., 2009). Together, available data suggest that imbalance in excitatory and inhibitory neurotransmitter contents in the brain significantly affect hypnotic and immobilizing actions of propofol and midazolam.

It must be emphasized, however, that the influence of GAD65 knockout is relatively small in terms of anesthetic sensitivity. In fact, hypnotic actions could be elicited in GAD65−/− mice with the use of higher concentrations of propofol and midazolam. The most likely interpretation of these findings is that other molecular targets may mediate behavioral responses to these agents. In this context, mutations in postsynaptic $GABA_A$ receptors have appeared to modulate *in vivo* propofol actions (Jurd et al., 2003). The mutation of asparagine to methionine (N265M) in the β3 subunit greatly reduces the ability of propofol and etomidate to cause LORR and eliminates their abilities to prevent response to painful stimuli, but has little effect on the actions of volatile anesthetics. In contract, the $GABA_A$ α1 subunit (S270) is a critical determinant that influences a variety of behaviors in the mouse in view of volatile anesthetic sensitivity (Homanics et al., 2005). These data show that postsynaptic $GABA_A$ receptors play more important roles with *in vivo* anesthetic potencies.

4.3. Increased extracellular GABA concentrations by GABA transporter 1 inhibition

The actions of synaptically released GABA are terminated by uptake into presynaptic terminals and surrounding glial cells via Na^+-dependent transporters. Molecular biological studies have cloned four subtypes of mouse GABA transporter (GAT): GAT-1, GT-2, GAT-3, and GAT-4 (Borden, 1996). NO-711 is a potent and selective GABA uptake inhibitor that exhibits the highest affinity for human GAT-1. Hybridization signals for GAT-1 mRNA have been observed over many regions of the rat brain, including the retina, olfactory bulb, neocortex, ventral pallidum, hippocampus, and cerebellum (Durkin et al., 1995), indicating that NO-711 induces an increase in endogenous GABA concentrations at many brain regions. However, the degree of increased GABA concentrations produced by NO-711 is difficult to determine. We estimated changes in GABA concentrations using two methods. First, we

confirmed physiologically that the amplitude of tonic conductance in cortical pyramidal neurons of brain slices from WT mice with NO-711 (3 mg/kg, ip) was greater than that of WT mice without apparent changes in IPSC amplitude, indicating that the tonic current is not a summation of IPSCs, but is instead attributable to continuous $GABA_A$ receptor activation by endogenous GABA. Second, we confirmed behaviorally that NO-711 (1.0–10 mg/kg, ip) dose-dependently increased the latency in the hot-plate test in WT mice and GAD65−/− mice (Kubo et al., 2009b). Judging from these data, NO-711 (1.0 mg/kg, ip) to GAD65−/− mice reinstated GABA levels similar to WT mice, because the latency was similar between groups. High-dose NO-711 (6.0–10 mg/kg) produced slight hypnotic actions in the absence of anesthetics (Kubo et al., 2009b). Together, we believe that NO-711 (3.0 mg/kg, ip) enhances ambient GABA contents without producing hypnotic properties.

One critical issue is the selectivity of the manipulations that were used to alter tonic but not phasic inhibition. Although the manipulations may well alter ambient GABA concentrations and thereby alter tonic inhibition, they may also alter phasic inhibition. Concerning this issue, we have previously confirmed that GAD65 gene knockout reduced tonic inhibition without affecting phasic inhibition (IPSCs) (Kubo et al., 2009a). Tian et al. (1999) have also reported that the frequency of sIPSCs was intact in retinal ganglion cells in GAD65−/− mice. Although we do not know the source of compensation for the synthesis of GABA being released, deleting GAD65 gene may have little effect on the GABA content of spontaneously released synaptic vesicles.

4.4. Molecular targets of general anesthetics: synaptic and extrasynaptic $GABA_A$ receptors

Growing evidence suggests that tonic $GABA_A$ receptors may be more important mediators of anesthetic-induced neural depression than phasic $GABA_A$ receptors (Orser, 2006). This concept is largely based on findings that tonic $GABA_A$ receptors are very sensitive to low concentrations of anesthetics. The continuous, non-desensitizing nature of tonic $GABA_A$ receptors could be expected to contribute to a larger charge transfer or shunting inhibition. The present study suggests that this notion may be true for some, but not all, types of general anesthetics. In contrast to the strong depressant effects produced by propofol (Bieda and MacIver, 2004) and thiopental (Bieda et al., 2009), actions of sevoflurane (0.23 mM) were not strong enough to alter discharge properties of layer V cortical neurons. In support of our data, isoflurane appears to enhance phasic $GABA_A$ inhibition, but does not enhance tonic $GABA_A$ receptors to depress synaptically evoked discharge of hippocampal CA1 neurons (Bieda et al., 2009). In addition, halothane at clinical concentrations (0.35 mM) has only minimal depressant effects on the postsynaptic membrane excitability of CA1 pyramidal cells (Sonner et al., 2003). AP discharge in response to depolarizing current injection is not altered by halothane, nor is the threshold, rise time or amplitude of spikes altered. Furthermore, Ogawa et al. (2011) have examined the effects of sevoflurane (0.3 mM) on extrasynaptic GABA receptors in mechanically dissociated hippocampal CA1 neurons. GABA (1 μM)-induced currents were enhanced by sevoflurane (138% of control), suggesting that extrasynaptic GABA receptors may contribute to the enhancement of the inhibitory responses to some degree. All over the result suggest that the role of ambient GABA concentrations (tonic conductance) may be different in volatile vs. intravenous anesthetics.

In this context, we are interested in the influence of ambient GABA contents on amnestic actions of anesthetics, because it has been shown that $GABA_A$ receptor α5 subunit null mutant mice had very little etomidate-induced amnesia, long-term potentiation, and tonic current augmentation (Cheng et al., 2006).

5. Conclusions

The present study provides *in vivo* evidence that genetic and pharmacological manipulations to alter ambient GABA concentrations have significant effects on the hypnotic and immobilizing actions of propofol and midazolam, whereas these manipulations minimally alter cellular and behavioral responses to sevoflurane.

Acknowledgments

This research was supported by Grants-in-Aid for Scientific Research from the Ministry of Education, Culture, Sports, Science and Technology of Japan to K.N. [#20390412], K.K. [#21890032], and Y.Y. [#20019010, 22300105]. This work was also supported by a Grant-in-Aid from the Japan Medical Association, Tokyo, Japan to K.N., JST, CREST and Takeda Science Foundation to Y.Y. The authors thank the staff at Institute of Experimental Animal Research, Gunma University Graduate School of Medicine, for technical assistance.

References

Bai, D., Zhu, G., Pennefather, P., Jackson, M.F., MacDonald, J.F., Orser, B.A., 2001. Distinct functional and pharmacological properties of tonic and quantal inhibitory postsynaptic currents mediated by gamma-aminobutyric acid (A) receptors in hippocampal neurons. Mol. Pharmacol. 59, 814–824.

Bieda, M.C., MacIver, M.B., 2004. Major role for tonic GABAA conductances in anesthetic suppression of intrinsic neuronal excitability. J. Neurophysiol. 92, 1658–1667.

Bieda, M.C., Su, H., MacIver, M.B., 2009. Anesthetics discriminate between tonic and phasic gamma-aminobutyric acid receptors on hippocampal CA1 neurons. Anesth. Analg. 108, 484–490.

Borden, L.A., 1996. GABA transporter heterogeneity: pharmacology and cellular localization. Neurochem. Int. 29, 335–356.

Borden, L.A., Murali Dhar, T.G., Smith, K.E., Weinshank, R.L., Branchek, T.A., Gluchowski, C., 1994. Tiagabine, SK&F 89976-A, CI-966, and NNC-711 are selective for the cloned GABA transporter GAT-1. Eur. J. Pharmacol. 269, 219–224.

Brickley, S.G., Cull-Candy, S.G., Farrant, M., 1996. Development of a tonic form of synaptic inhibition in rat cerebellar granule cells resulting from persistent activation of GABAA receptors. J. Physiol. 497, 753–759.

Chen, X., Sirois, J.E., Lei, Q., Talley, E.M., Lynch 3rd, C., Bayliss, D.A., 2005. HCN subunit-specific and cAMP-modulated effects of anesthetics on neuronal pacemaker currents. J. Neurosci. 25, 5803–5814.

Cheng, V.Y., Martin, L.J., Elliott, E.M., Kim, J.H., Mount, H.T., Taverna, F.A., Roder, J.C., Macdonald, J.F., Bhambri, A., Collinson, N., Wafford, K.A., Orser, B.A., 2006. Alpha5GABAA receptors mediate the amnestic but not sedative-hypnotic effects of the general anesthetic etomidate. J. Neurosci. 26, 3713–3720.

Durkin, M.M., Smith, K.E., Borden, L.A., Weinshank, R.L., Branchek, T.A., Gustafson, E.L., 1995. Localization of messenger RNAs encoding three GABA transporters in rat brain: an in situ hybridization study. Brain Res. Mol. Brain Res. 33, 7–21.

Erlander, M.G., Tillakaratne, N.J., Feldblum, S., Patel, N., Tobin, A.J., 1991. Two genes encode distinct glutamate decarboxylases. Neuron 7, 91–100.

Franks, N.P., 2006. Molecular targets underlying general anaesthesia. Br. J. Pharmacol. 147, S72–S81.

Franks, N.P., Lieb, W.R., 1996. Temperature dependence of the potency of volatile general anesthetics: implications for in vitro experiments. Anesthesiology 84, 716–720.

Franks, N.P., Lieb, W.R., 1998. Which molecular targets are most relevant to general anaesthesia? Toxicol. Lett. 100–101, 1–8.

Glykys, J., Mody, I., 2007. Activation of GABAA receptors: views from outside the synaptic cleft. Neuron 56, 763–770.

Hemmings Jr., H.C., Akabas, M.H., Goldstein, P.A., Trudell, J.R., Orser, B.A., Harrison, N.L., 2005. Emerging molecular mechanisms of general anesthetic action. Trends Pharmacol. Sci. 26, 503–510.

Homanics, G.E., Elsen, F.P., Ying, S.W., Jenkins, A., Ferguson, C., Sloat, B., Yuditskaya, S., Goldstein, P.A., Kralic, J.E., Morrow, A.L., Harrison, N.L., 2005. A gain-of-function mutation in the GABA receptor produces synaptic and behavioral abnormalities in the mouse. Genes Brain Behav. 4, 10–19.

Ishizeki, J., Nishikawa, K., Kubo, K., Saito, S., Goto, F., 2008. Amnestic concentrations of sevoflurane inhibit synaptic plasticity of hippocampal CA1 neurons through gamma-aminobutyric acid-mediated mechanisms. Anesthesiology 108, 447–456.

Jurd, R., Arras, M., Lambert, S., Drexler, B., Siegwart, R., Crestani, F., Zaugg, M., Vogt, K.E., Ledermann, B., Antkowiak, B., Rudolph, U., 2003. General anesthetic actions in vivo strongly attenuated by a point mutation in the GABA(A) receptor beta3 subunit. FASEB J. 17, 250–252.

Kash, S.F., Johnson, R.S., Tecott, L.H., Noebels, J.L., Mayfield, R.D., Hanahan, D., Baekkeskov, S., 1997. Epilepsy in mice deficient in the 65-kDa isoform of glutamic acid decarboxylase. Proc. Natl. Acad. Sci. USA 94, 14060–14065.

Kash, S.F., Tecott, L.H., Hodge, C., Baekkeskov, S., 1999. Increased anxiety and altered responses to anxiolytics in mice deficient in the 65-kDa isoform of glutamic acid decarboxylase. Proc. Natl. Acad. Sci. USA 96, 1698–1703.

Kitamura, A., Marszalec, W., Yeh, J.Z., Narahashi, T., 2003. Effects of halothane and propofol on excitatory and inhibitory synaptic transmission in rat cortical neurons. J. Pharmacol. Exp. Ther. 304, 162–171.

Kubo, K., Nishikawa, K., Hardy-Yamada, M., Ishizeki, J., Yanagawa, Y., Saito, S., 2009a. Altered responses to propofol, but not ketamine, in mice deficient in the 65-kilodalton isoform of glutamate decarboxylase. J. Pharmacol. Exp. Ther. 329, 592–599.

Kubo, K., Nishikawa, K., Ishizeki, J., Hardy-Yamada, M., Yanagawa, Y., Saito, S., 2009b. Thermal hyperalgesia via supraspinal mechanisms in mice lacking glutamate decarboxylase (GAD) 65. J. Pharmacol. Exp. Ther. 331, 162–169.

Mascia, M.P., Machu, T.K., Harris, R.A., 1996. Enhancement of homomeric glycine receptor function by long-chain alcohols and anaesthetics. Br. J. Pharmacol. 119, 1331–1336.

Mihic, S.J., Ye, Q., Wick, M.J., Koltchine, V.V., Krasowski, M.D., Finn, S.E., Mascia, M.P., Valenzuela, C.F., Hanson, K.K., Greenblatt, E.P., Harris, R.A., Harrison, N.L., 1997. Sites of alcohol and volatile anaesthetic action on GABA (A) and glycine receptors. Nature 389, 385–389.

Moe, M.C., Berg-Johnsen, J., Larsen, G.A., Kampenhaug, E.B., Vinje, M.L., 2003. The effect of isoflurane and sevoflurane on cerebrocortical presynaptic Ca^{2+} and protein kinase C activity. J. Neurosurg. Anesthesiol. 15, 209–214.

Namchuk, M., Lindsay, L., Turck, C.W., Kanaani, J., Baekkeskov, S., 1997. Phosphorylation of serine residues 3, 6, 10, and 13 distinguishes membrane anchored from soluble glutamic acid decarboxylase 65 and is restricted to glutamic acid decarboxylase 65alpha. J. Biol. Chem. 272, 1548–1557.

Nishikawa, K., MacIver, M.B., 2001. Agent-selective effects of volatile anesthetics on GABAA receptor-mediated synaptic inhibition in hippocampal interneurons. Anesthesiology 94, 340–347.

Nishikawa, K., Harrison, N.L., 2003. The actions of sevoflurane and desflurane on the gamma-aminobutyric acid receptor type A: effects of TM2 mutations in the alpha and beta subunits. Anesthesiology 99, 678–684.

Nishikawa, K., Kubo, K., Ishizeki, J., Takazawa, T., Saito, S., Goto, F., 2005. The interaction of noradrenaline with sevoflurane on GABA(A) receptor-mediated inhibitory postsynaptic currents in the rat hippocampus. Brain Res. 1039, 153–161.

Ogawa, S.K., Tanaka, E., Shin, M.C., Kotani, N., Akaike, N., 2011. Volatile anesthetic effects on isolated GABA synapses and extrasynaptic receptors. Neuropharmacology 60, 701–710.

Orser, B.A., 2006. Extrasynaptic $GABA_A$ receptors are critical targets for sedative-hypnotic drugs. J. Clin. Sleep Med. 2, S12–S18.

Pitler, T.A., Alger, B.E., 1992. Cholinergic excitation of GABAergic interneurons in the rat hippocampal slice. J. Physiol. 450, 127–142.

Quasha, A.L., Eger 2nd, E.I., Tinker, J.H., 1980. Determination and applications of MAC. Anesthesiology 53, 315–334.

Quinlan, J.J., Homanics, G.E., Firestone, L.L., 1998. Anesthesia sensitivity in mice that lack the beta3 subunit of the gamma-aminobutyric acid type A receptor. Anesthesiology 88, 775–780.

Rudolph, U., Antkowiak, B., 2004. Molecular and neuronal substrates for general anaesthetics. Nat. Rev. Neurosci. 5, 709–720.

Semyanov, A., Walker, M.C., Kullmann, D.M., Silver, R.A., 2004. Tonically active GABA A receptors: modulating gain and maintaining the tone. Trends Neurosci. 27, 262–269.

Sirois, J.E., Lei, Q., Talley, E.M., Lynch 3rd, C., Bayliss, D.A., 2000. The TASK-1 two-pore domain K^+ channel is a molecular substrate for neuronal effects of inhalation anesthetics. J. Neurosci. 20, 6347–6354.

Sonner, J.M., Antognini, J.F., Dutton, R.C., Flood, P., Gray, A.T., Harris, R.A., Homanics, G.E., Kendig, J., Orser, B., Raines, D.E., Rampil, I.J., Trudell, J., Vissel, B., Eger 2nd, E.I., 2003. Inhaled anesthetics and immobility: mechanisms, mysteries, and minimum alveolar anesthetic concentration. Anesth. Analg. 97, 718–740.

Stork, O., Ji, F.Y., Kaneko, K., Stork, S., Yoshinobu, Y., Moriya, T., Shibata, S., Obata, K., 2000. Postnatal development of a GABA deficit and disturbance of neural functions in mice lacking GAD65. Brain Res. 865, 45–58.

Stucke, A.G., Zuperku, E.J., Tonkovic-Capin, V., Krolo, M., Hopp, F.A., Kampine, J.P., Stuth, E.A., 2005. Sevoflurane depresses glutamatergic neurotransmission to brainstem inspiratory premotor neurons but not postsynaptic receptor function in a decerebrate dog model. Anesthesiology 103, 50–56.

Takazawa, T., Furue, H., Nishikawa, K., Uta, D., Takeshima, K., Goto, F., Yoshimura, M., 2009. Actions of propofol on substantia gelatinosa neurones in rat spinal cord revealed by in vitro and in vivo patch-clamp recordings. Eur. J. Neurosci. 29, 518–528.

Tian, N., Petersen, C., Kash, S., Baekkeskov, S., Copenhagen, D., Nicoll, R., 1999. The role of the synthetic enzyme GAD65 in the control of neuronal gamma-aminobutyric acid release. Proc. Natl. Acad. Sci. USA 96, 12911–12916.

Wu, X.S., Sun, J.Y., Evers, A.S., Crowder, M., Wu, L.G., 2004. Isoflurane inhibits transmitter release and the presynaptic action potential. Anesthesiology 100, 663–670.

Yamada, J., Furukawa, T., Ueno, S., Yamamoto, S., Fukuda, A., 2007. Molecular basis for the GABAA receptor-mediated tonic inhibition in rat somatosensory cortex. Cereb. Cortex 17, 1782–1787.

Yamamoto, T., Yamamoto, E., Tashiro, F., Sato, T., Noso, S., Tamura, S., Yanagawa, Y., Miyazaki, J., 2004. Development of autoimmune diabetes in glutamic acid decarboxylase 65 (GAD65) knockout NOD mice. Diabetologia 47, 221–224.

Yanagawa, Y., Kobayashi, T., Ohnishi, M., Kobayashi, T., Tamura, S., Tsuzuki, T., Sanbo, M., Yagi, T., Tashiro, F., Miyazaki, J., 1999. Enrichment and efficient screening of ES cells containing a targeted mutation: the use of DT-A gene with the polyadenylation signal as a negative selection marker. Transgenic Res. 8, 215–221.

J Anesth (2011) 25:855–859
DOI 10.1007/s00540-011-1236-y

ORIGINAL ARTICLE

Comparison of recovery times from rocuronium-induced muscle relaxation after reversal with three different doses of sugammadex and succinylcholine during electroconvulsive therapy

Yuji Kadoi · Hiroko Hoshi · Akiko Nishida · Shigeru Saito

Received: 22 May 2011 / Accepted: 5 September 2011 / Published online: 24 September 2011

Abstract
Purpose This study was conducted to compare recovery times from rocuronium-induced muscle relaxation after reversal with three different doses of sugammadex with succinylcholine during electroconvulsive therapy (ECT).
Methods Seventeen patients who were scheduled to undergo ECT were studied. Anesthesia was induced by use of propofol (1.0 mg/kg) followed by either succinylcholine (SCC) (1 mg/kg) or rocuronium (0.6 mg/kg). Assisted mask ventilation was initiated with 100% oxygen. After T1 was assessed as being zero by neuromuscular monitoring, an electroshock stimulus was applied bilaterally. Patients receiving rocuronium were infused with 16, 8, or 4 mg/kg sugammadex immediately after the seizure stopped to reverse the muscle relaxation. Neuromuscular monitoring was continued until recovery of the train-of-four ratio to 0.9 at the tibial nerve in the leg. The times to recovery of T1 to 10 and 90% with both relaxants were compared.
Results The time to recovery of T1 to 90% after 16 mg/kg sugammadex was shorter than that in subjects treated with SCC ($p = 0.046$), whereas that after 4 mg/kg sugammadex was longer than that in subjects treated with SCC (SCC group: 429 ± 65 s, 16 mg/kg sugammadex group: 387 ± 63 s*, 8 mg/kg sugammadex group: 462 ± 66 s, 4 mg/kg sugammadex group: 563 ± 45 s*,#; *$p < 0.05$ compared with SCC, #$p < 0.01$ compared with 16 mg/kg sugammadex).
Conclusions This study demonstrates the efficacy of rocuronium–sugammadex as an alternative to SCC for muscle relaxation during ECT, and indicates that 8 mg/kg sugammadex produces equally rapid recovery from rocuronium muscular relaxation compared with spontaneous recovery from 1 mg/kg SCC during ECT.

Keywords Electroconvulsive therapy · Muscle relaxant · Rocuronium · Sugammadex · Succinylcholine

Y. Kadoi (✉) · H. Hoshi · A. Nishida · S. Saito
Department of Anesthesiology, Gunma University, School of Medicine, 3-39-22 Showa-Machi, Maebashi, Gunma 371-8511, Japan
e-mail: kadoi@med.gunma-u.ac.jp

Introduction

Succinylcholine (SCC) is commonly used as a muscle relaxant during electroconvulsive therapy (ECT) because of its rapid onset and short duration of action [1]. However, SCC has many side effects, for example myalgia, a small increase in plasma potassium, and increase in intra-gastric and intra-ocular pressures [1].

Sugammadex has recently been introduced as a fast-acting, selective relaxant-binding agent that was designed to rapidly reverse rocuronium-induced neuromuscular block. Lee et al. [2, 3] reported that reversal of profound rocuronium (1.0–1.2 mg/kg)-induced neuromuscular block with a large dose of sugammadex (16 mg/kg) was significantly faster than spontaneous recovery from SCC. Previously, we showed the potential benefit of using rocuronium (0.6 mg/kg)–sugammadex (16 mg/kg) as an alternative to SCC (1 mg/kg) for muscle relaxation during ECT [4]. A large dose of rocuronium (1.0–1.2 mg/kg) is usually not needed for muscle relaxation during ECT, as shown in our previous study [4] and that of others [1]. Hence, we speculated that a slightly smaller dose of sugammadex would be required for equally rapid recovery from 0.6 mg/kg rocuronium-induced muscle relaxation as from relaxation with 1 mg/kg SCC.

The purpose of this study was to determine the dose of sugammadex that would produce an equal recovery time

from 0.6 mg/kg rocuronium-induced muscle relaxation as from spontaneous recovery from relaxation with 1 mg/kg SCC during ECT.

Materials and methods

Informed consent was obtained from patients or their families. All protocols were approved by the local Institutional Clinical Study Committee and the Institutional Review Board. Seventeen patients who were scheduled to undergo ECT were studied. None of the patients had a history of cardiovascular, hepatic, renal, or neuromuscular disease, or were obese (BMI >35).

Anesthetic management

All patients underwent at least 10 sessions of ECT (three times per week at 1 or 2-day intervals). To avoid induction of the parasympathetic reflex, the patients received atropine (0.01 mg/kg IM) 30 min before the ECT procedure.

Data measured during the procedure included blood pressure (BP), heart rate, oxygen saturation (SpO_2; measured by pulse oximetry on the left or right index finger), end-expiratory partial pressure of carbon dioxide (end-tidal CO_2:$PetCO_2$) at the nostrils (Capnomac Ultima; Datex, Helsinki, Finland) and electrocardiogram (ECG; lead II). Measurements were initiated before ECT and were terminated at the end of the procedure.

Anesthesia was induced by use of propofol (1.0 mg/kg intravenously over 5 s), followed by either SCC (1 mg/kg intravenously) or rocuronium (0.6 mg/kg intravenously) over 5 s, followed by a 10-ml saline bolus. Assisted mask ventilation was initiated with 100% oxygen. After T1 was assessed as being zero by neuromuscular monitoring, an electroshock stimulus was applied bilaterally for 5 s.

$PetCO_2$ was maintained at 30–35 mmHg and the SpO_2 value was maintained above 98% by manual mask assistance throughout the therapy. Patients who received rocuronium were infused with 16, 8, or 4 mg/kg sugammadex with a 10-ml saline bolus immediately after the seizure stopped.

During the first and second ECT sessions, we confirmed that 1 mg/kg propofol and 1 mg/kg SCC could provide adequate anesthetic conditions and muscle relaxation to all patients. In addition, the intensity of the ECT stimulus required to achieve a minimum seizure duration of more than 20 s was determined during these sessions.

All patients received 1 mg/kg SCC as the muscle relaxant agent for first three of the subsequent ECT sessions and 0.6 mg/kg rocuronium during the next three sessions. In the remaining sessions (from 7 to 10 or 12 sessions) 1 mg/kg SCC was used as the muscle relaxant agent. When rocuronium was used as the muscle relaxant, patients received one of three sugammadex dosages (16, 8, or 4 mg/kg), with a 10-ml saline bolus immediately after the seizure stopped, the dose of sugammadex to be used in a particular session being decided by a lottery system. Administration of sugammadex was in a non-blinded manner. Electroencephalographic (EEG) seizure duration was recorded by a two-channel EEG after administration of the electrical stimulus.

Neuromuscular assessment

Neuromuscular monitoring was performed using the TOF-watch SX (Organon, Roseland, NJ, USA). The tibial nerve in the leg was supramaximally stimulated at the inferolateral aspect of the medial malleolus with square pulses of 0.2-ms duration, delivered as train-of-four (TOF) pulses, at intervals of 15 s. The resulting contractions of the great toe muscles were quantified by an acceleromyographic monitor. Calibration was performed and baseline responses were recorded after propofol administration and before muscle relaxant administration. A 50-Hz titanic stimulus was applied for 5 s and followed after 1 min by TOF stimulation every 15 s. When the response to TOF stimulation was stable, calibration and supramaximal stimulation were ensured by the in-built calibration function. Neuromuscular monitoring was continued until recovery of the TOF ratio to 0.9. Following the protocol of our previous study [4], we compared the time to recovery of T1 to 10 and 90% between relaxants. T1 was zero in all patients when sugammadex was administered. We used recovery of T1 to 10% (instead of TOF ratio) for its simplicity, its common usefulness between depolarizing and non-depolarizing relaxants, and because the TOF ratio has uncertain significance with a single dose of SCC.

Patients were also assessed for clinical signs such as the time interval between the first spontaneous breath and administration of muscle relaxant and the time to opening of eyes to verbal commands.

Statistical analysis

All data are expressed as mean ± standard deviation (SD). Before the study was started, sample size was evaluated. The sample size was calculated on the basis of the hypothesis that recovery of T1 to 10% with 4 mg/kg sugammadex would be prolonged to 60 s compared to that with SCC [4]. The sample size provided 80% power to detect a 20% difference between 4 mg/kg sugammadex and the SCC groups with a 5% probability of a type II error. A paired t test was used for comparison of the two groups. For multiple comparisons, one-way factorial ANOVA and the Bonferroni test were used for the

comparison. Values of $p < 0.05$ were considered statistically significant.

Calculations were performed by Stat View 5.0 software (Abacus Concepts, Berkeley, CA, USA).

Results

Patient age, height, and weight were 58 ± 14 years, 157 ± 7 cm, 57 ± 10 kg, respectively. Seven of the 17 patients were male.

Table 1 shows the comparison between the effects of SCC and rocuronium in terms of time from the start of administration of neuromuscular blocking agent to a T1 of zero. There was no significant difference between the groups.

Table 2 shows the time from commencement of administration of neuromuscular blocking agents to recovery of T1 to 10 and 90%, seizure duration, and time to first spontaneous breath in the two groups. The time to recovery of T1 to 90% in subjects treated with 16 mg/kg sugammadex was shorter than that in subjects treated with SCC ($p = 0.046$), and the time to recovery of T1 to both 10 and 90% in subjects treated with 4 mg/kg sugammadex was longer than that in subjects treated with SCC ($p < 0.01$). The time to first spontaneous breath in subjects treated with 16 mg/kg sugammadex was shorter than that in subjects treated with SCC ($p = 0.045$), and the time to first spontaneous breath in subjects treated with 4 mg/kg sugammadex was longer than that in subjects treated with SCC ($p < 0.01$). No significant difference in seizure duration was found among the four groups.

No adverse effects, such as nausea, vomiting, myalgia, or headache occurred with either relaxant. In addition, no symptoms of recurarization, for example respiratory depression (indicated by a decrease in SpO_2 less than 90% without supplementary oxygen supply) were seen in any of the patients treated with rocuronium–sugammadex (4, 8, or 16 mg/kg sugammadex) during the observation period of up to 12 h after the administration of rocuronium–sugammadex, when the patients were in the ward.

Table 1 Time from commencement of administration of neuromuscular blocking agents to a T1 of zero with each drug

	SCC	Rocuronium
Time to T1 of 0% (s)	109 ± 28	123 ± 28
p value	0.13	

Discussion

This study showed that:

1. the onset of action of 0.6 mg/kg rocuronium is equivalent to that of 1 mg/kg SCC for muscle relaxation during ECT; and
2. 8 mg/kg sugammadex is adequate for reversal of muscle relaxation induced by 0.6 mg/kg rocuronium during ECT.

Although Trollor and Sachdev [5] suggested the possible safety of the use of SCC in cases with neuroleptic malignant syndrome, SCC is thought to be a potent trigger for malignant hyperthermia (MH) [2]. Moreover, use of SCC is associated with a variety of adverse events and contraindications [2]. To avoid these, some researchers examined other neuromuscular agents, for example vecuronium [6, 7], mivacurium [8–10], rapacuronium [11] and rocuronium [12] during ECT. Kelly and Brull [10] demonstrated the safety of mivacurium as an alternative to SCC. In contrast, Cheam et al. [8] reported that a low dose of mivacurium was less effective than SCC. Another study of the safety of vecuronium reported that vecuronium shortened seizure duration and prolonged anesthetic time [6].

Rocuronium is potentially useful for muscle relaxation during ECT. However, before our previous study [4] there

Table 2 Time from commencement of administration of neuromuscular blocking agents to recovery of T1 to 10 and 90%, seizure duration, time to first spontaneous breath, and interval between rocuronium and sugammadex administration with each drug

	Recovery of T1 to 10% (s)	Recovery of T1 to 90% (s)	Time to first spontaneous breath (s)	Seizure duration (s)	Time from administration of rocuronium to administration of sugammadex (s)
SCC	310 ± 38	429 ± 65	273 ± 43	36 ± 6	
Sugammadex, 16 mg/kg	280 ± 54	387 ± 63*	233 ± 53*	38 ± 4	134 ± 7
Sugammadex, 8 mg/kg	324 ± 68	462 ± 66	267 ± 69	40 ± 7	132 ± 8
Sugammadex, 4 mg/kg	407 ± 74*,#	563 ± 45*,#	360 ± 59*,#	39 ± 5	134 ± 8

SCC, succinylcholine

* $p < 0.05$ compared with SCC

# $p < 0.05$ compared with sugammadex 16 mg/kg group

was only one report evaluating the effects of rocuronium versus SCC on clinical recovery from ECT [12]. Turkkal et al. [12] reported that although the time to first spontaneous breath was longer in the rocuronium group than in the SCC group, no significant differences were detected between the two groups in terms of eye opening, head lift, or tongue depressor testing. However, the dosage of rocuronium used in the study of Turkkal et al. [12] was relatively small (0.3 mg/kg), which is thought to be inadequate for muscular paralysis, because a dose of 0.3 mg/kg IV is rocuronium's ED_{50} dose for the laryngeal adductor muscles, this being half of the recommended intubating dose for rocuronium. Rocuronium (0.6–1.2 mg/kg) typically produces complete neuromuscular block within 2 min, compared with an average of 1 min with 1 mg/kg SCC [13]. High-dose rocuronium (1.0–1.2 mg/kg) has been recommended by some researchers as an effective alternative to SCC for rapid sequence induction. However, a meta-analysis of the Cochrane Review [14] concluded that intubation conditions do not statistically significantly differ with the administration of SCC and rocuronium when propofol is used to rapidly induce anesthesia. Indeed, in this study, no difference in the time from commencement of administration of neuromuscular blocking agents to T1 zero was found between the two groups. Hence, doses of 0.6 mg/kg rocuronium and 1 mg/kg SCC are appropriate for muscle relaxation during ECT.

Sluga et al. [15] compared tracheal intubation conditions with the use of 0.6 mg/kg rocuronium and 1 mg/kg SCC in emergency cases and showed that the time interval from injection of the neuromuscular blocking agents to the cessation of a visible motor response to continuous single-twitch nerve stimulation of the ulnar nerve was shorter in the SCC group (median time 40 s) than in the rocuronium group (median time 70 s). Although there was a tendency towards a longer interval between commencement of administration of neuromuscular blocking agents and T1 zero in the rocuronium group in this study, the difference between the two groups was not significant. The possible cause of this difference, as we previously showed [16], is that the onset of action of muscle relaxants is greatly affected by cardiac output before injection. Another possibility is that Sluga et al. [15] selected 1.5 mg/kg propofol with 2 μg/kg fentanyl for anesthetic induction. The difference in the anesthetic regime may also be responsible for the different results.

Lee et al. [3] compared the time required for sugammadex reversal of profound rocuronium-induced neuromuscular block with time to spontaneous recovery after SCC. In their study, either 1.2 mg/kg rocuronium or 1 mg/kg SCC was used for block of neuromuscular transmission and facilitation of tracheal intubation. Sugammadex (16 mg/kg) was administered 3 min after rocuronium administration. Mean times to recovery of T1 to 90% were significantly faster in the rocuronium–sugammadex group than in the SCC group. Hence, they concluded that reversal of profound high-dose rocuronium-induced neuromuscular block (1.2 mg/kg) with 16 mg/kg sugammadex was significantly faster than spontaneous recovery from 1 mg/kg SCC. In an earlier report from Gijsenbergh et al. [17] with an intubating dose of 0.6 mg/kg rocuronium, the TOF ratio returned to 0.9 within 2 min after administration of 8.0 mg/kg sugammadex given 3 min after the administration of rocuronium. Pühringer et al. [13] examined the dose-dependent effects of sugammadex for reversal of profound neuromuscular block. Sugammadex (2, 4, 8, 12, or 16 mg/kg) was administrated 3 min after the administration of 1.0 or 1.2 mg/kg rocuronium. The time to recovery of the TOF ratio to 0.9 with sugammadex was faster in a dose-dependent manner. These two reports showed that although the recovery speed of the TOF ratio to 0.9 with sugammadex was dose-dependent, its efficacy was unchanged. Our study showed that although 16 mg/kg sugammadex resulted in the fastest recovery of the TOF ratio to 0.9 in the case of 0.6 mg/kg rocuronium, 8 mg/kg sugammadex had equipotent effects on the recovery of the TOF ratio to 0.9 compared with the use of SCC during ECT.

Batistaki et al. [18] reported successful anesthetic management of a patient with pseudocholinesterase deficiency by use of rocuronium reversed by sugammadex in a series of ECT sessions. In a preliminary report, we showed the potential efficacy of the use of rocuronium–sugammadex as a muscle relaxant during ECT [4]. Hence, rocuronium–sugammadex could also be useful for muscle relaxation during ECT for patients for whom the use of SCC is contraindicated. Our report implies that a combination of rocuronium–sugammadex, using 0.6 mg/kg rocuronium, may be adequate for inducing muscle paralysis during ECT. In addition, 8 mg/kg sugammadex produced adequate recovery from the muscular relaxation induced by 0.6 mg/kg rocuronium during ECT.

In this study, the patients were administered a combination of rocuronium–sugammadex repeatedly once a day for a week during the study. Although this repeated administration may possibly have adverse effects on the patients, we did not find any adverse effects (nausea, vomiting, prolongation of the QTc interval), and more specifically, recurarization, with any of the three doses of sugammadex. Batistaki et al. [18] reported that a combination of rocuronium–sugammadex used every 48 h for 8 consecutive ECT sessions proved to be effective and safe in a situation where SCC was contraindicated. Our study also confirms the potential usefulness of rocuronium–sugammadex for muscle relaxation during ECT for patients for whom the use of SCC is contraindicated, for example those with severe osteoporosis, amyotrophic lateral sclerosis, and a history of neuroleptic syndrome.

Another consideration is that the combination of rocuronium–sugammadex is eliminated by the kidney, so that it is possible that its elimination could be prolonged in patients with impaired renal function, which could induce adverse effects in these patients. All patients included in this study had normal renal function, as shown by normal serum creatinine and BUN levels. However, care should be taken when using sugammadex for patients with impaired renal function. Use of the combination of rocuronium–sugammadex would also be disadvantageous compared with SCC in cases where re-use of rocuronium is required immediately after administration of sugammadex.

In conclusion, we demonstrated the efficacy of rocuronium–sugammadex as an alternative to SCC for muscle relaxation during ECT and showed that 8 mg/kg SG has equipotent recovery time from muscular relaxation compared with 1 mg/kg SCC during ECT.

Acknowledgments The authors wish to thank Forte (Tokyo, Japan) for assistance with manuscript preparation in English. This study was supported in part by grants to Dr Kadoi (no. 21591998) from the Japanese Ministry of Education, Culture, Sports, Science and Technology.

Conflict of interest No authors have any conflicts of interest in association with this article.

References

1. Kadoi Y, Saito S. Anesthetic considerations for electroconvulsive therapy-especially hemodynamic and respiratory management. Curr Psychiatry Rev. 2009;5:276–86.
2. Lee C. Goodbye suxamethonium!. Anaesthesia. 2009;64:73–81.
3. Lee C, Jahr JS, Candiotti KA, Warriner B, Zornow MH, Naguib M. Reversal of profound neuromuscular block by sugammadex administered three minutes after rocuronium: a comparison with spontaneous recovery from succinylcholine. Anesthesiology. 2009;110:1020–5.
4. Hoshi H, Kadoi Y, Kamiyama J, Nishida A, Saito H, Taguchi M, Saito S. Use of rocuronium–sugammadex, an alternative to succinylcholine, as a muscle relaxant during electroconvulsive therapy. J Anesth. 2011;25:286–90.
5. Trollor JN, Sachdev PS. Electroconvulsive treatment of neuroleptic malignant syndrome: a review and report of cases. Aust N Z J Psychiatry. 1999;33:650–9.
6. Nishiyama M, Togashi H. Effects of anesthetic agents on seizure duration and hemodynamics in electroconvulsive therapy. Masui (Jpn J Anesthesiol). 2009;58:1266–9. (in Japanese with English abstract).
7. Setoyama K, Hirata T, Saeki H, Morimoto Y, Tsuruta S, Matsumoto M, Sakabe T. Anesthetic management for electroconvulsive therapy in the patients with a history of neuroleptic malignant syndrome. Masui (Jpn J Anesthesiol). 2009;58:633–6. (in Japanese with English abstract).
8. Cheam EW, Critchley LA, Chui PT, Yap JC, Ha VW. Low dose mivacurium is less effective than succinylcholine in electroconvulsive therapy. Can J Anesth. 1999;46:49–51.
9. Janis K, Hess J, Fabian JA, Gillis M. Substitution of mivacurium for succinylcholine for ECT in elderly patients. Can J Anesth. 1995;42:612–3.
10. Kelly D, Brull SJ. Neuroleptic malignant syndrome and mivacurium: a safe alternative to succinylcholine? Can J Anaesth. 1994;41:845–9.
11. Kadar AG, Kramer BA, Barth MC, White PF. Rapacuronium: an alternative to succinylcholine for electroconvulsive therapy. Anesth Analg. 2001;92:1171–2.
12. Turkkal DC, Gokmen N, Yildiz A, Iyilikci L, Gokel E, Sagduyu K, Gunerli A. A cross-over, post-electroconvulsive therapy comparison of clinical recovery from rocuronium versus succinylcholine. J Clin Anesth. 2008;20:589–93.
13. Pühringer FK, Rex C, Sielenkämper AW, Claudius C, Larsen PB, Prins ME, Eikermann M, Khuenl-Brady KS. Reversal of profound, high-dose rocuronium-induced neuromuscular blockade by sugammadex at two different time points: an international, multicenter, randomized, dose-finding, safety assessor-blinded, phase II trial. Anesthesiology. 2008;109:188–97.
14. Perry J, Lee J, Wells G. Rocuronium versus succinylcholine for rapid sequence induction intubation. In: The Cochrane Library. Issue 3. Hoboken: Wiley; 2004.
15. Sluga M, Ummenhofer W, Studer W, Siegemund M, Marsch SC. Rocuronium versus succinylcholine for rapid sequence induction of anesthesia and endotracheal intubation: a prospective, randomized trial in emergent cases. Anesth Analg. 2005;101:1356–61.
16. Matsumoto N, Tomioka A, Sato T, Kawasaki M, Kadoi Y, Saito S. Relationship between cardiac output and onset of succinylcholine chloride action in electroconvulsive therapy patients. J ECT. 2009;25:246–9.
17. Gijsenbergh F, Ramael S, Houwing N, van Iersel T. First human exposure of Org 25969, a novel agent to reverse the action of rocuronium bromide. Anesthesiology. 2005;103:695–703.
18. Batistaki C, Kesidis K, Apostolaki S, Kostopanagiotou G. Rocuronium antagonized by sugammadex for series of electroconvulsive therapy (ECT) in a patient with pseudocholinesterase deficiency. J ECT. 2011;27:e47–8.

Skeletal Radiol (2012) 41:163–167
DOI 10.1007/s00256-011-1144-0

SCIENTIFIC ARTICLE

Correlation between T2 relaxation time and intervertebral disk degeneration

Hiroyuki Takashima · Tsuneo Takebayashi · Mitsunori Yoshimoto · Yoshinori Terashima · Hajime Tsuda · Kazunori Ida · Toshihiko Yamashita

Received: 2 February 2011 / Revised: 24 February 2011 / Accepted: 27 February 2011 / Published online: 23 March 2011

Abstract
Objective Magnetic resonance T2 mapping allows for the quantification of water and proteoglycan content within tissues and can be used to detect early cartilage abnormalities as well as to track the response to therapy. The goal of the present study was to use T2 mapping to quantify intervertebral disk water content according to the Pfirrmann classification.
Materials and methods This study involved 60 subjects who underwent lumbar magnetic resonance imaging (a total of 300 lumbar disks). The degree of disk degeneration was assessed in the midsagittal section on T2-weighted images according to the Pfirrmann classification (grades I to V). Receiver operating characteristic (ROC) analysis was performed among grades to determine the cut-off values.
Results In the nucleus pulposus, T2 values tended to decrease with increasing grade, and there was a significant difference in T2 values between each grade from grades I to IV. However, there was no significant difference in T2 values in the anterior or posterior annulus fibrosus. T2 values according to disk degeneration level classification were as follows: grade I (>116.8 ms), grade II (92.7–116.7 ms), grade III (72.1–92.6 ms), grade IV (<72.0 ms).
Conclusion T2 values decreased with increasing Pfirrmann classification grade in the nucleus pulposus, likely reflecting a decrease in proteoglycan and water content. Thus, T2 value-based measurements of intervertebral disk water content may be useful for future clinical research on degenerative disk diseases.

Keywords Lumbar disk degeneration · T2 relaxation time · Classification

H. Takashima · T. Takebayashi (✉) · M. Yoshimoto · Y. Terashima · H. Tsuda · K. Ida · T. Yamashita
Department of Orthopedic Surgery, School of Medicine, Sapporo Medical University, South-1, West-16, Chuo-ku, Sapporo, Hokkaido 060–8543, Japan
e-mail: takebaya@sapmed.ac.jp

H. Takashima
e-mail: takashima@sapmed.ac.jp

Introduction

In developed countries, low back pain is one of the most frequent reasons for working-age disability. There are a number of causes of low back pain [1–3], with degenerative disk disease thought to be the most common [4–6]. The intervertebral disks comprise the nucleus pulposus at the center and the annulus fibrosus at the periphery. The nucleus pulposus is composed of ionized water, proteoglycans, and collagen. The annulus fibrosus connects to the vertebra, which adjoins the fibrous tissue consisting of type 1 collagen [7–9].

Magnetic resonance imaging (MRI) is the most useful modality for characterization of disk lesions. Signal variation of the disks on T2-weighted images reflects age and degeneration and allows for the determination of disk degeneration. Specifically, since signal strength in the MRI is related to water and proteoglycan content, changes in MRI signal strength in the nucleus pulposus can indicate disk degeneration [10, 11]. Disk degeneration has been classified by T2-weighted images using the system described by Pfirrmann et al. [12], but since this classification is based on visual evaluation, the quantification of degeneration using this strategy is unclear.

Among MRI technologies, MRI T2 mapping allows quantification of water content and can be used to detect early cartilage abnormalities and track the response to therapy [13, 14]. Because the T2 value is a quantitative

Table 1 Classification of intervertebral disk degeneration as reported by Pfirrmann et al. [12]

Grade	Structure	Distinction of the nucleus and annulus	Signal intensity	Height of the intervertebral disk
I	Homogeneous, bright white	Clear	Hyperintense, isointense to CSF	Normal
II	Heterogeneous with or without horizontal bands	Clear	Hyperintense, isointense to CSF	Normal
III	Heterogeneous, gray	Unclear	Intermediate	Normal to slightly decreased
IV	Heterogeneous, gray or black	Lost	Intermediate or hypointense	Normal to moderately decreased
V	Heterogeneous, black	Lost	Hypointense	Collapsed disk space

parameter that varies with collagen and water content in cartilage and in the intervertebral disk [15–18], this modality may also be useful to characterize the etiology of lower back pain and disk degeneration [19]. In these previous studies correlating T2 value with disk degeneration, the boundaries of the classification based on quantitative evaluation have not been fully investigated. Further, a disk degeneration classification that is quantifiable may be of value for research purposes related to disk abnormalities. Thus, the goal of this study was to use T2 mapping to quantify intervertebral disk water content according to the Pfirrmann classification and propose an objective borderline for the classification based on T2 value.

Materials and methods

Written informed consent was obtained from all patients, and all protocols were approved by the ethics committee. This study involved 60 volunteers (25 male, 35 female, average age, 53.3 years; range, 23–83 years) who underwent MRI of the lumbar spine (a total of 300 lumbar disks) because of low back pain and leg numbness and tingling, including pain. Equipment consisted of a spine coil with a GE Signa HDx 1.5 T (GE Healthcare, Milwaukee, WI, USA). T2-weighted sagittal images (TR 4,000 ms, TE 102 ms, receive band width [RBW] ±31.25 kHz, field of view [FOV] 24 cm, matrix 384×288, slice thickness/gap 4 mm/1 mm, number of excitations [NEX] 4, total scan time 3 min and 4 s) were obtained, and a radiologist blindly classified the grade of disk degeneration as grade I to V in the midsagittal section according to the Pfirrmann classification (Table 1); meanwhile, he was not involved in the measurement of T2 values.

Next, a T2 map was created using the T2 values in the midsagittal section from sagittal sections centered on the lumbar midline region with optimized 8 echo multi-spin echo (TR/ first echo TE, last echo TE, 1,000/14.8, 118.6, RBW ±15.63 kHz, FOV 22 cm, matrix 320×256, slice thickness/gap 4 mm/4 mm, 5 slices, NEX 2, total scan time 8 min and 34 s) obtained with an Advantage Workstation (version 4.4, Functool; GE Healthcare, Milwaukee, WA, USA). However, the first echo from the multi-spin system was excluded to minimize the effect of the stimulated echo. The T2 map was calculated in each pixel from the signal intensity (SI) in the respective TE using the following calculating formula:

$$SI = e^{-TE/T2}$$

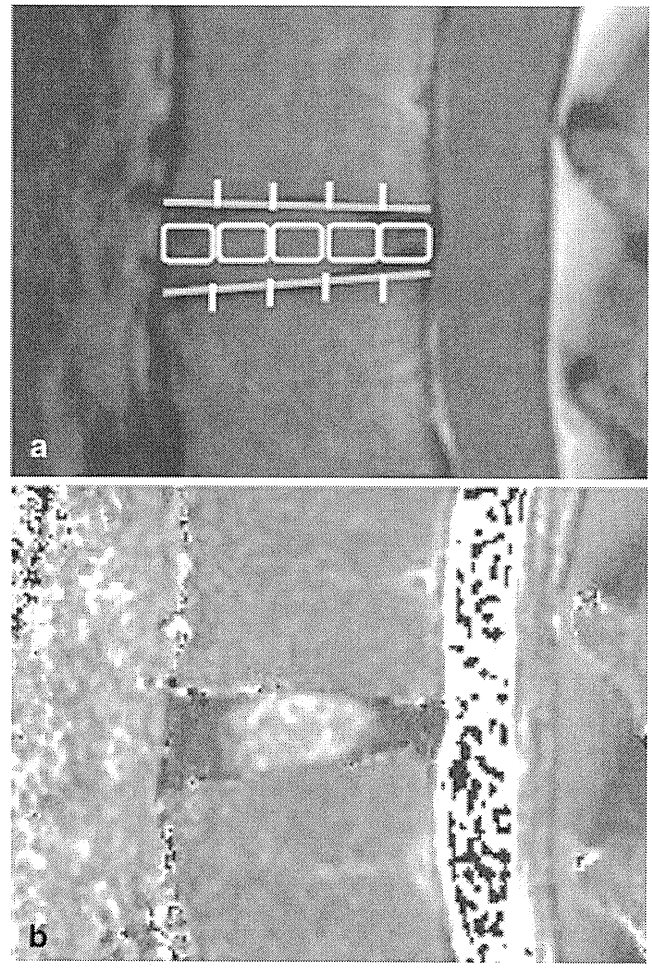

Fig. 1 Measurement of the intervertebral disk. **a** Second echo image on original image of T2 mapping. Disks were divided into five equal areas, designating the front fifth or the anterior annulus fibrosus, the middle fifth of the nucleus pulposus, and the last fifth of the posterior annulus fibrosus. **b** T2 mapping. In the same ROI as in **a**, we measured the mean values

For measurement, disks were divided into five equal areas, designating the front fifth of the anterior annulus fibrosus, the middle fifth of the nucleus pulposus, and the last fifth of the posterior annulus fibrosus. The mean values in the regions of interest (ROI) were measured (Fig. 1). MedCalc (version 10.2.0.0; MedCalc Software, Mariakerke, Belgium) was used to analyze the T2 values for each respective grade and to conduct a comparative investigation. Furthermore, in order to determine the T2 boundary values between the Pfirrmann classification grades in the nucleus pulposus region, receiver operating characteristic (ROC) analysis was performed between each grade. The Mann–Whitney U test was used for significant difference testing, with $p<0.05$ indicating statistical significance.

Results

The T2-weighted image-based Pfirrmann grade classification consisted of the following: grade I, 42 disks; grade II, 61 disks; grade III, 67 disks; grade IV, 77 disks; and grade V, 53 disks. The T2 values measured in each grade, comprising the anterior annulus fibrosus, nucleus pulposus, and posterior annulus fibrosus, are shown in Fig. 2. In the nucleus pulposus, T2 values tended to decrease with increasing grades, and T2 values were significantly different when comparing grades I to IV, but not when comparing grades IV and V. No significant difference was observed between the grades in either the anterior or posterior annulus fibrosus. The difference in T2 values between grade IV and grade V in the nucleus pulposus and annulus fibrosus was small and not statistically significant.

Receiver-operating characteristic analysis between each grade in the nucleus pulposus yielded the cut-off values illustrated in Fig. 3. However, since there was a significant difference in T2 values between grades IV and V, values from these two categories were combined into one group. The T2 cut-off value between grades I and II was 116.8 ms, which corresponded to a sensitivity, specificity, and area under the ROC curve (AUC) of 64.5%, 90.5%, and 0.831 respectively. The cut-off value, sensitivity, specificity, and AUC between grades II and III were 92.7 ms, 68.7%, 96.8%, and 0.879 respectively, and those between grades III and IV were 72.1 ms, 80.0%, 85.1%, and 0.886 respectively. The T2 values based on the disk degeneration level scale from these results are shown in Table 2.

Discussion

Intervertebral disk water content decreases with age and degeneration [20]. When evaluating disk degeneration, it is common to classify the amount of water in the intervertebral disks, as reflected by the T2-weighted image signal intensity, according to the method described by Pfirrmann et al. Although T2-weighted images are used to evaluate for disk degeneration in clinical settings [21–23], the signal intensity cannot be measured as absolute values because of a number of factors, including signal detection and signal amplification [24]. Thus, the goal of the present study was to use T2 mapping to measure T2 values of the water content in intervertebral disks according to the Pfirrmann classification.

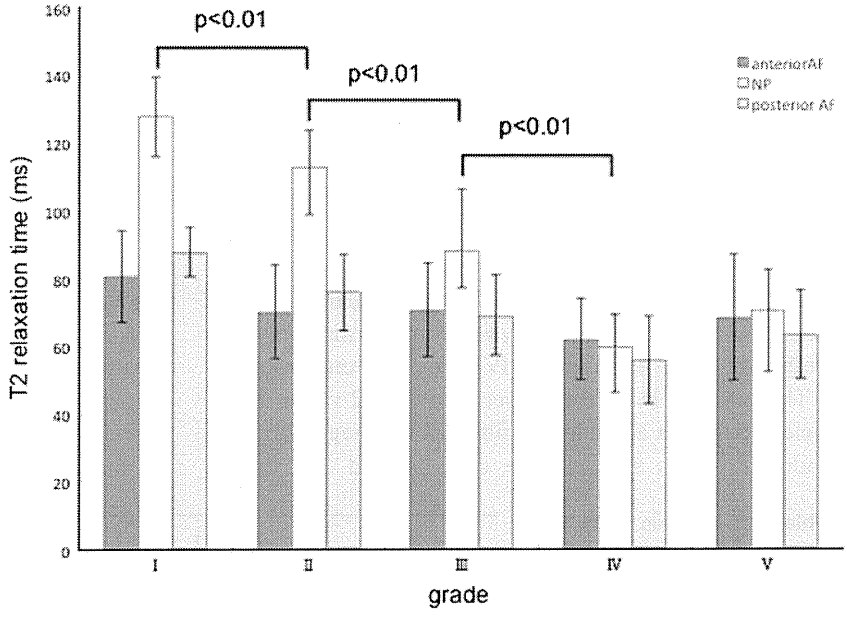

Fig. 2 Relationship between grade and T2 value. In the nucleus pulposus there is a tendency indicated for T2 values to decrease in progression with the grades, and there was a significant difference discerned between each grade from grade I to IV, but there was no significant difference between grade IV and V. No significant difference was observed between the grades in either the anterior or posterior annulus fibrosus either. Furthermore, the difference between grade IV and grade V T2 values in the nucleus pulposus and annulus fibrosus was small, and no statistically significant difference was discerned

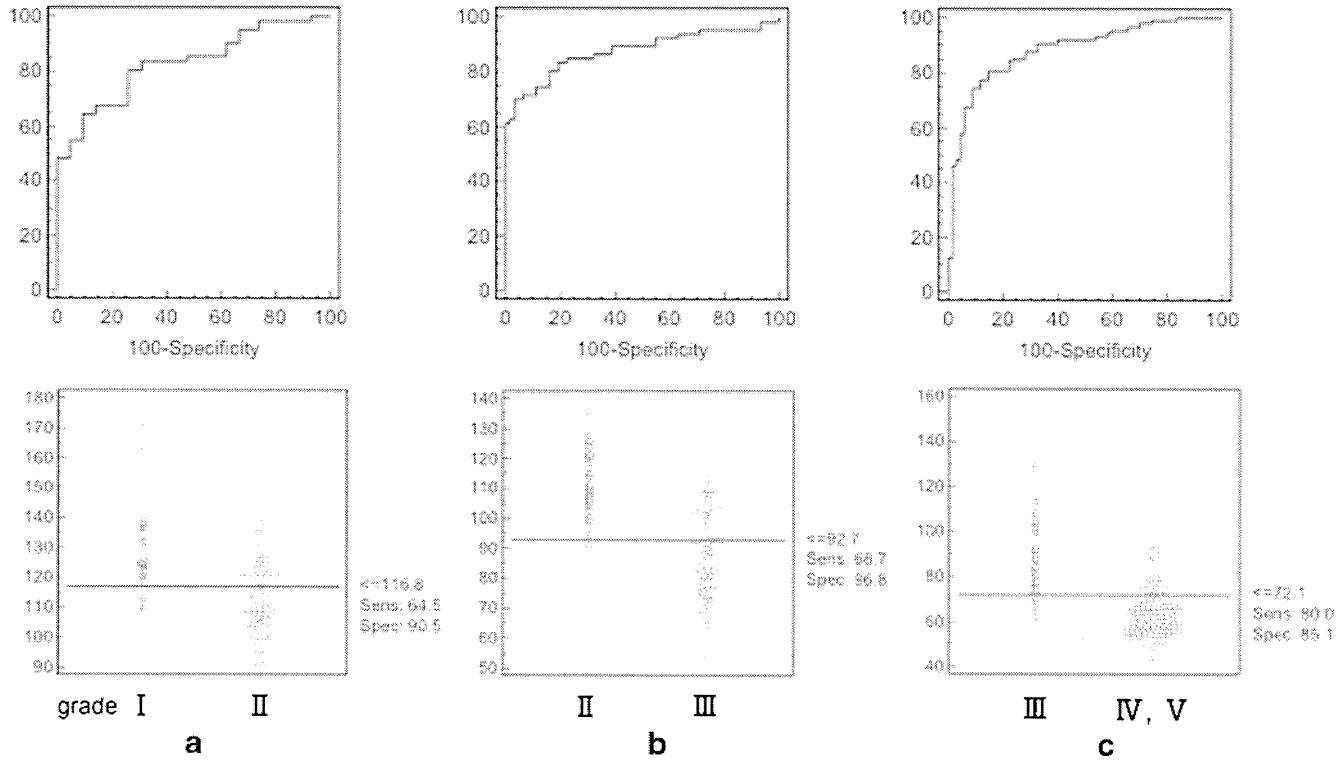

Fig. 3 A receiver-operating characteristic (ROC) curve between each grade in the nucleus pulposus and a cut-off point. We obtained the most accurate point from the ROC curve as the cut-off value. **a** The T2 cut-off value between grades I and II was found to be 116.8 ms, sensitivity 64.5%, specificity 90.5%, and AUC 0.831. **b** The values between grades II and III were 92.7 ms, 68.7%, 96.8%, and 0.879. **c** Between grades III and IV/V the values were 72.1 ms, 80.0%, 85.1%, and 0.886

T2 is the damping constant in T2 signal intensity on MRI, which is not image parameter-reliant. This parameter reflects an environment of molecules produced in the intervertebral disks, including protein, neutral fat, collagen, and other solutes [25]. In past reports that measured T2 values in intervertebral disks, the values varied from 63 ms to 123 ms [21] and from 51±10 to 91±19 [26], which is consistent with results from the present study.

In the present study, the T2 values tended to decrease in response to increasing Pfirrmann classification grade in the nucleus pulposus. This may reflect a reduction in proteoglycan and water content [10, 11]. However, grade V of the Pfirrmann classification was noteworthy for the height of the intervertebral disk. Therefore, we did not discern a significant difference in T2 values between grades IV and V. It may be difficult to distinguish between grades IV and V using T2 values. As a result, further analysis was performed only after combining values from grades IV and V into one group.

There was little difference between the T2 values of the nucleus pulposus and annulus fibrosus with regard to these grades. Previous studies have demonstrated that the T2 values in the nucleus pulposus and annulus fibrosus decrease in proportion to disk degeneration, and, ultimately, differences in T2 signal intensity between these two structures approach zero [6, 16, 21], which is consistent with results from the present study. Thus, comparison of T2 values between the nucleus pulposus and annulus fibrosus may also aid in the evaluation of disk degeneration.

Receiver operating characteristic analysis between each grade of the nucleus pulposus yielded cut-off values for quantification of disk degeneration via T2 signal intensity. The cut-off points obtained from the ROC curve can be determined with approximate reliability from the AUC values. The AUC values of 0.9–1.0 denote high accuracy, 0.9–0.7, moderate accuracy, and 0.5–0.7, low accuracy. The AUC values in this study were all within the moderate accuracy range, indicating an intermediate level of reliability. These data indicate that this T2 value-based grade scale is useful, with a high degree of objectivity.

This study has several limitations. First, the reliability for ROC analysis of the AUC values based on visual evaluation was moderately accurate. Greater accuracy could

Table 2 Correlation with T2 relaxation time with intervertebral disk degeneration

	Grade I	Grade II	Grade III	Grade IV
Nucleus pulposus	116.8 ms~	92.7 ms~116.7 ms	72.1 ms~92.6 ms	~72.0 ms

be achieved if ROI analysis were not visually based, but only based on T2 value measurements. Second, distinguishing between the nucleus pulposus and the annulus fibrosus in the setting of advanced degeneration is difficult, which complicates the setting of the ROI. Although we divided the intervertebral disks into five areas with an anterior and posterior annulus fibrosus in order to decrease variance between the measurements, the validity of this measuring method has not been evaluated.

The selection of ROIs in most previous reports was done manually. The reproducibility of this technique is suspect because of the poor differentiation of the central nuclear region from the peripheral annulus. Our selection of ROIs was not manual, but based on measuring small areas divided equally. This technique is more reliably reproducible than the manual approach and also has minimal measurement bias.

In summary, T2 values decreased with increasing Pfirrmann classification grade in the nucleus pulposus, likely reflecting a decrease in proteoglycan and water content. We proposed the boundaries of the classification based on quantitative evaluation. Thus, T2 value-based measurements of intervertebral disk water content may be useful for future clinical research on degenerative disk diseases.

Acknowledgement

Conflict of interest The authors declare that there is no conflict of interest.

References

1. Andersson GB. Epidemiology of low back pain. Acta Orthop Scand Suppl. 1998;281:28–31.
2. Benneker LM, Heini PF, Anderson SE, Alini M, Ito K. Correlation of radiographic and MRI parameters to morphological and biochemical assessment of intervertebral disc degeneration. Eur Spine J. 2005;14(1):27–35.
3. Praemer A, Furner S, Rice DP, American Academy of Orthopaedic Surgeons. Musculoskeletal conditions in the United States. 1st ed. Park Ridge, IL: American Academy of Orthopaedic Surgeons, 1992
4. Paajanen H, Erkintalo M, Parkkola R, Salminen J, Kormano M. Age-dependent correlation of low-back pain and lumbar disc regeneration. Arch Orthop Trauma Surg. 1997;116(1–2):106–7.
5. Salminen JJ, Erkintalo MO, Pentti J, Oksanen A, Kormano MJ. Recurrent low back pain and early disc degeneration in the young. Spine (Phila Pa 1976). 1999;24(13):1316–21.
6. Weinstein JN, Gordon SL, Buckwalter JA, American Academy of Orthopaedic Surgeons. Low back pain: a scientific and clinical overview. 1st ed. Rosemont, IL: American Academy of Orthopaedic Surgeons, 1996
7. Hardy PA. Intervertebral disks on MR images: variation in signal intensity with the disk-to-magnetic field orientation. Radiology. 1996;200(1):143–7.
8. Ludescher B, Effelsberg J, Martirosian P, Steidle G, Markert B, Claussen C, et al. T2- and diffusion-maps reveal diurnal changes of intervertebral disc composition: an in vivo MRI study at 1.5 Tesla. J Magn Reson Imaging. 2008;28(1):252–7.
9. Nightingale T, MacKay A, Pearce RH, Whittall KP, Flak B. A model of unloaded human intervertebral disk based on NMR relaxation. Magn Reson Med. 2000;43(1):34–44.
10. Urban JP, McMullin JF. Swelling pressure of the lumbar intervertebral discs: influence of age, spinal level, composition, and degeneration. Spine (Phila Pa 1976). 1988;13(2):179–87.
11. Zou J, Yang H, Miyazaki M, Morishita Y, Wei F, McGovern S, et al. Dynamic bulging of intervertebral discs in the degenerative lumbar spine. Spine (Phila Pa 1976). 2009;34(23):2545–50.
12. Pfirrmann CW, Metzdorf A, Zanetti M, Hodler J, Boos N. Magnetic resonance classification of lumbar intervertebral disc degeneration. Spine (Phila Pa 1976). 2001;26(17):1873–8.
13. Friedrich KM, Shepard T, de Oliveira VS, Wang L, Babb JS, Schweitzer M, et al. T2 measurements of cartilage in osteoarthritis patients with meniscal tears. AJR Am J Roentgenol. 2009;193(5): W411–5.
14. Mosher TJ, Dardzinski BJ. Cartilage MRI T2 relaxation time mapping: overview and applications. Semin Musculoskelet Radiol. 2004;8(4):355–68.
15. Weidenbaum M, Foster RJ, Best BA, Saed-Nejad F, Nickoloff E, Newhouse J, et al. Correlating magnetic resonance imaging with the biochemical content of the normal human intervertebral disc. J Orthop Res. 1992;10(4):552–61.
16. Blumenkrantz G, Zuo J, Li X, Kornak J, Link TM, Majumdar S. In vivo 3.0-tesla magnetic resonance T1rho and T2 relaxation mapping in subjects with intervertebral disc degeneration and clinical symptoms. Magn Reson Med. 2010;63(5):1193–1200.
17. Karakida O, Ueda H, Ueda M, Miyasaka T. Diurnal T2 value changes in the lumbar intervertebral discs. Clin Radiol. 2003;58 (5):389–92.
18. Perry J, Haughton V, Anderson PA, Wu Y, Fine J, Mistretta C. The value of T2 relaxation times to characterize lumbar intervertebral disks: preliminary results. AJNR Am J Neuroradiol. 2006;27(2):337–42.
19. Boos N, Wallin A, Gbedegbegnon T, Aebi M, Boesch C. Quantitative MR imaging of lumbar intervertebral disks and vertebral bodies: influence of diurnal water content variations. Radiology. 1993;188(2):351–4.
20. Krueger EC, Perry JO, Wu Y, Haughton VM. Changes in T2 relaxation times associated with maturation of the human intervertebral disk. AJNR Am J Neuroradiol. 2007;28(7):1237–41.
21. Chiu EJ, Newitt DC, Segal MR, Hu SS, Lotz JC, Majumdar S. Magnetic resonance imaging measurement of relaxation and water diffusion in the human lumbar intervertebral disc under compression in vitro. Spine (Phila Pa 1976). 2001;26(19):E437–44.
22. Gundry CR, Fritts HM. Magnetic resonance imaging of the musculoskeletal system. VIII. The spine, section 2. Clin Orthop Relat Res. 1997;343:260–71.
23. Modic MT, Pavlicek W, Weinstein MA, Boumphrey F, Ngo F, Hardy R, et al. Magnetic resonance imaging of intervertebral disk disease. Clinical and pulse sequence considerations. Radiology. 1984;152(1):103–11.
24. Watanabe A, Benneker LM, Boesch C, Watanabe T, Obata T, Anderson SE. Classification of intervertebral disk degeneration with axial T2 mapping. AJR Am J Roentgenol. 2007;189(4):936–42.
25. Marinelli NL, Haughton VM, Munoz A, Anderson PA. T2 relaxation times of intervertebral disc tissue correlated with water content and proteoglycan content. Spine (Phila Pa 1976). 2009;34 (5):520–4.
26. Marinelli NL, Haughton VM, Anderson PA. T2 Relaxation times correlated with stage of lumbar intervertebral disk degeneration and patient age. AJNR Am J Neuroradiol. 2010;31(7):1278–82.

ARTHRITIS & RHEUMATISM
Vol. 64, No. 1, January 2012, pp 198–203
DOI 10.1002/art.33324

BRIEF REPORT

Lack of a Chondroprotective Effect of Cyclooxygenase 2 Inhibition in a Surgically Induced Model of Osteoarthritis in Mice

Atsushi Fukai, Satoru Kamekura, Daichi Chikazu, Takumi Nakagawa, Makoto Hirata, Taku Saito, Yoko Hosaka, Toshiyuki Ikeda, Kozo Nakamura, Ung-il Chung, and Hiroshi Kawaguchi

Objective. **To investigate the chondroprotective effect of cyclooxygenase 2 (COX-2) inhibition in experimental osteoarthritis (OA).**

Methods. **The expression of prostaglandin E_2 synthetic enzymes was examined by immunostaining of tibial cartilage from mice with surgically induced knee joint instability and from OA patients undergoing total knee arthroplasty. The effect of orally administered celecoxib (10 mg/kg/day and 30 mg/kg/day) or vehicle alone in mice was examined 12 weeks after the induction of OA. To investigate the involvement of COX-1 and COX-2 in OA development, we also created the model in COX-1–homozygous-knockout (*Ptgs1*$^{-/-}$) mice and COX-2–homozygous-knockout (*Ptgs2*$^{-/-}$) mice. OA severity was assessed using a grading system developed by our group and by the Osteoarthritis Research Society International scoring system.**

Results. **In mouse and human OA cartilage, the expression of the inducible enzymes COX-2 and microsomal prostaglandin E synthase 1 (mPGES-1) was enhanced, while that of the constitutive enzymes COX-1, cytosolic PGES, and mPGES-2 was suppressed. Daily celecoxib treatment did not prevent cartilage degradation or osteophyte formation during OA development in the mouse model. Furthermore, neither *Ptgs1*$^{-/-}$ mice nor *Ptgs2*$^{-/-}$ mice exhibited any significant difference in OA development as compared to wild-type littermates.**

Conclusion. **The two COX enzymes differ in terms of regulation of their expression during OA development. Nevertheless, experiments using inhibitor and genetic deficiency demonstrated a lack of chondroprotective effect of COX-2 inhibition in the mouse surgical OA model.**

Prostaglandin E_2 (PGE_2) is thought to be a possible therapeutic target in osteoarthritis (OA), since it acts as one of the major catabolic mediators involved in degradation of joint cartilage in vitro and is produced in abundance in OA cartilage (1). In the biosynthesis of PGE_2, 3 enzymes have been identified: phospholipase A_2, cyclooxygenase (COX), and PGE synthase (PGES) (2). There are 2 isoforms of COX: COX-1 (encoded by *Ptgs1*) and COX-2 (*Ptgs2*), and 3 isoforms of PGES: microsomal PGES-1 (mPGES-1) (*Ptges*), mPGES-2 (*Ptges2*), and cytosolic PGES (cPGES) (*Ptges3*). COX-1, mPGES-2, and cPGES are expressed constitutively in various tissues and function to maintain their homeostasis, whereas COX-2 and mPGES-1 are induced by various stimuli during catabolic and inflammatory processes.

Although nonsteroidal antiinflammatory drugs (NSAIDs), which inactivate COX enzymes, are commonly used as symptom-modifying treatment to suppress pain and inflammation in OA, the notion of their chondroprotective effects as disease-modifying drugs remains controversial (3). A human genetic study identified the *PTGS2* gene variant as being involved in the risk of knee OA, suggesting the importance of the COX-2 signal in disease pathogenesis (4). Likewise, previous in vitro and ex vivo studies have shown that celecoxib, a representative selective COX-2 inhibitor, has chondroprotective effects in cultures of chondrocytes and cartilage (5,6). However, in vivo evaluation by the same group failed to demonstrate a beneficial effect of celecoxib in the canine model of OA (7), and a recent randomized controlled trial in OA patients, also con-

Supported by the Japanese Ministry of Education, Culture, Sports, Science, and Technology (Grants-in-Aid for Scientific Research 18209047 and 19109007).

Atsushi Fukai, MD, PhD, Satoru Kamekura, MD, PhD, Daichi Chikazu, MD, PhD, Takumi Nakagawa, MD, PhD, Makoto Hirata, MD, PhD, Taku Saito, MD, PhD, Yoko Hosaka, MD, Toshiyuki Ikeda, MD, Kozo Nakamura, MD, PhD, Ung-il Chung, MD, PhD, Hiroshi Kawaguchi, MD, PhD: University of Tokyo, Tokyo, Japan.

Address correspondence to Hiroshi Kawaguchi, MD, PhD, Sensory and Motor System Medicine, Faculty of Medicine, University of Tokyo, Hongo 7-3-1, Bunkyo, Tokyo 113-8655, Japan. E-mail: kawaguchi-ort@h.u-tokyo.ac.jp.

Submitted for publication March 15, 2011; accepted in revised form August 30, 2011.

ducted by that group, similarly failed to replicate the chondroprotective effect of celecoxib (8).

Since risk factors for OA, as identified to date in epidemiologic studies, have been related to accumulated mechanical loading on joints, experimental OA models with surgical induction of knee joint instability have been developed in several animals (9). Among them, the mouse is currently the ideal animal for molecular studies because of recent progress in mouse genetics and the availability of transgenic and knockout mice. Hence, models of mechanical instability–induced OA in mouse knee joints, which are reproducible and resemble human OA, have been established using microsurgical techniques (9). In the present study, we used the mouse model to investigate the chondroprotective effect of COX-2 inhibition achieved by celecoxib treatment and by knockout of the *Ptgs2* gene.

MATERIALS AND METHODS

Animals and materials. All experiments were performed according to the protocol approved by the Animal Care and Use Committee of the University of Tokyo. *Ptgs1*$^{+/-}$ and *Ptgs2*$^{+/-}$ mice (10,11) (obtained from The Jackson Laboratory) and their wild-type littermates were generated by mating the *Ptgs1*$^{+/-}$ mice and *Ptgs2*$^{+/-}$ mice, respectively, that were maintained on a C57BL6/129S hybrid background. Interleukin-1α (IL-1α)– and IL-1β–double-knockout mice, tumor necrosis factor α (TNFα)–knockout mice, and control wild-type mice of the same C57BL/6 background were kindly provided by Dr. Yoichiro Iwakura (University of Tokyo). Human samples were obtained from OA patients undergoing total knee arthroplasty; all human donors had provided written informed consent as approved by the Ethics Committee of the University of Tokyo.

OA model and drug administration in mice. The surgical procedure to establish experimental OA was performed on 8-week-old mice as previously described (12). Briefly, the animals were placed under general anesthesia and the medial collateral ligament was transected and the medial meniscus removed using a surgical microscope. A sham operation was performed on the contralateral knee joint using the same approach, with no ligament transection or meniscectomy. The animals were then allowed unrestricted activity and food and water ad libitum. For the studies of celecoxib treatment, celecoxib (10 mg/kg or 30 mg/kg; Pfizer) in 0.5% carboxymethylcellulose and distilled water or the vehicle carboxy-

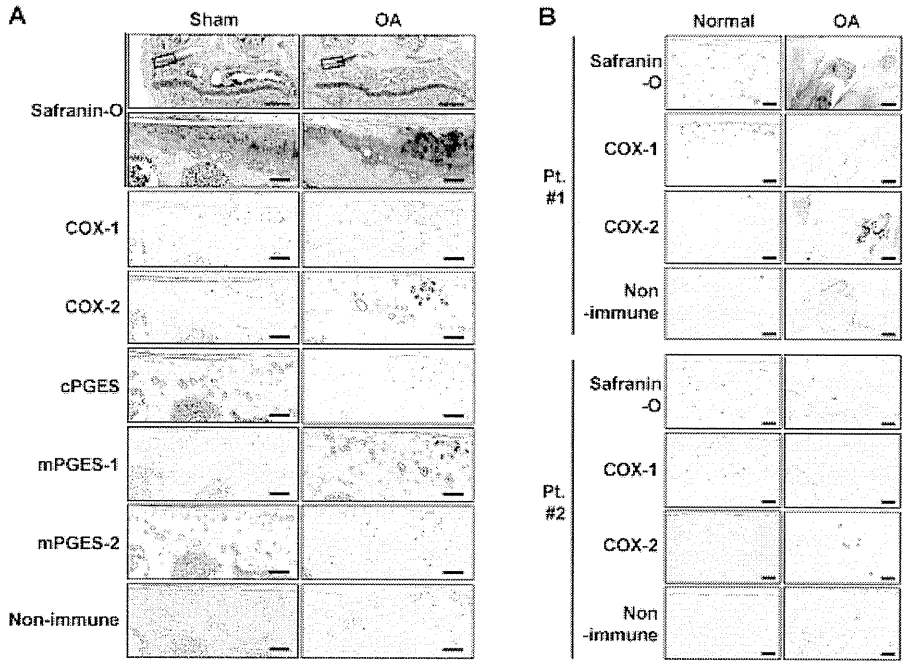

Figure 1. Expression of prostaglandin E_2 (PGE_2) synthetic enzymes in osteoarthritic (OA) joint cartilage from mice and humans. **A,** Safranin O staining and immunohistochemical staining with antibodies to cyclooxygenase 1 (COX-1), COX-2, cytosolic PGE synthase (cPGES), microsomal PGES 1 (mPGES-1), mPGES-2, and nonimmune IgG (control) in the medial portion of tibial cartilage from mice 8 weeks after surgical induction of OA in the right knee joints. Sham surgery was performed on the left knee joints. The lower Safranin O staining images are higher-magnification views of the boxed areas in the upper Safranin O staining images. **B,** Safranin O staining and immunostaining with antibodies to COX-1, COX-2, and nonimmune IgG (control) in normal and OA regions of tibial cartilage from 2 patients (Pt.) undergoing total knee arthroplasty. Bars in the top panels of **A** = 200 μm; other bars = 20 μm.

methylcellulose alone was administered orally once per day at a volume of 2 ml/kg body weight.

Histologic analysis. At various time points after surgery, the mice were killed, and the entire knee joints were dissected and fixed for 4 hours in 4% paraformaldehyde with phosphate buffered saline. The specimens were decalcified for 2 weeks with 10% EDTA. After the specimens were dehydrated with increasing concentrations of ethanol and embedded in paraffin, 4 μm of the frontal section was cut from the joints. Sections were stained with Safranin O–fast green. OA severity was assessed by a single observer who was blinded with regard to the experimental group, using our original grading system (12) and the Osteoarthritis Research Society International (OARSI) scoring system (13).

Immunohistochemical staining was performed on deparaffinized sections, and signal was detected with a CSAII Biotin-free Tyramide Signal Amplication System (Dako). The sections were incubated with polyclonal rabbit antibodies against COX-1, COX-2, cPGES, mPGES-1, mPGES-2, or nonimmune rabbit IgG (Cayman Chemical) at a dilution of 1:200. Sections were counterstained with methyl green.

Statistical analysis. Group means were compared by analysis of variance, and the significance of differences was determined by post hoc testing with Bonferroni adjustment. *P* values less than 0.05 were considered significant.

RESULTS

We initially investigated the expression of PGE_2 synthetic enzymes in mouse tibial cartilage during knee OA development, using the surgical OA model (12) (Figure 1A). Expression of the inducible enzymes COX-2 and mPGES-1 was barely detectable in the sham-operated cartilage, while these enzymes were increased focally in chondrocytes around the contact area of the OA cartilage. In contrast, although the constitutive enzymes COX-1, cPGES, and mPGES-2 were widely detected in the sham-operated cartilage, they were decreased in the OA cartilage. In human tibial cartilage samples obtained as surgical specimens from 2 OA patients undergoing total knee arthroplasty, COX-2 was expressed in chondrocytes from the OA cartilage, although it was barely detectable in normal cartilage in the surgical specimens from the same patients (Figure 1B). Expression of COX-1, in contrast, was decreased in the OA cartilage.

We then examined the effects of daily administration of celecoxib on OA development in the mouse OA model (Figure 2). We used two dosages of celecoxib, i.e., a dosage that was comparable to clinical usage (10 mg/kg/day) and one that was higher (30 mg/kg/day), and compared the results with those in vehicle-treated mice with OA as well as in vehicle-treated sham-operated mice. All mice (n = 32) survived the observation period of 12 weeks after surgery without disorders in major

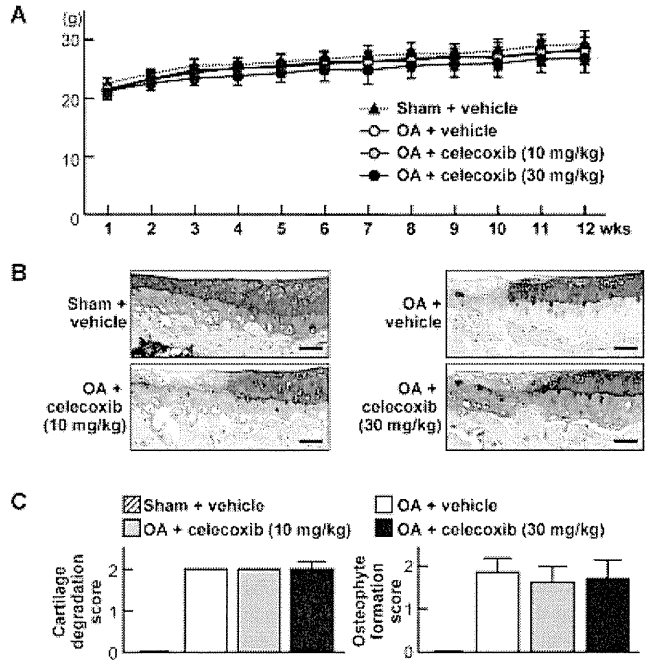

Figure 2. Effects of orally administered celecoxib (10 mg/kg/day and 30 mg/kg/day) on osteoarthritis (OA) development during the 12 weeks after surgical induction of OA at the age of 8 weeks. A group of mice with OA treated with vehicle alone and a sham-operated group treated with vehicle alone were also studied. **A,** Body weight at each week. There was no significant difference between any of the groups at any time point. **B,** Safranin O staining of the medial portion of tibial cartilage 12 weeks after surgery, in a representative knee joint sample from each group. Bars = 20 μm. **C,** Quantification of OA development by our grading system. There was no significant difference between any of the groups. Results obtained using the Osteoarthritis Research Society grading system were the same (data not shown). Values in **A** and **C** are the mean ± SD of 8 mice per group.

organs, and there was no significant difference in body weight among the 4 groups ($P > 0.05$) (Figure 2A). Although the tibial cartilage underwent degradation during the 12 weeks after OA surgery as compared to sham surgery, OA development was not altered by treatment with celecoxib at either dosage (Figure 2B). Quantification by our grading system (12) (Figure 2C) and the OARSI score (13) (data not shown) confirmed that celecoxib treatment did not prevent cartilage degradation or osteophyte formation during OA development.

Although celecoxib treatment failed to demonstrate a chondroprotective effect, it remains unknown whether celecoxib reaches the knee joints in a sufficient concentration or whether mouse chondrocytes are sensitive to human celecoxib. Hence, we next examined the involvement of COX-1 and COX-2 in OA development by establishing the surgical OA model in *Ptgs1*$^{-/-}$and

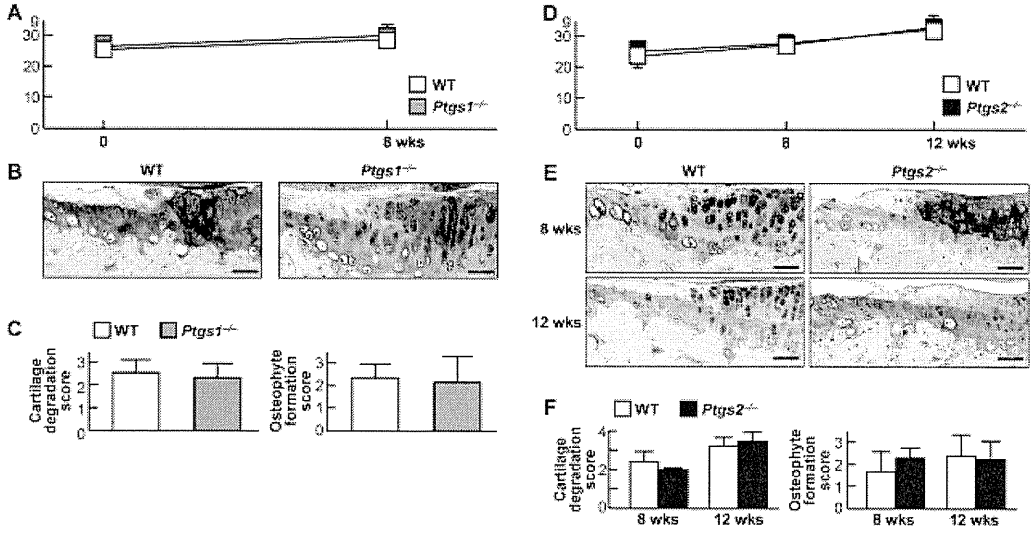

Figure 3. Effects of genetic deficiency of *Ptgs1* and *Ptgs2* on osteoarthritis (OA) development 8 and 12 weeks after surgical induction of OA at the age of 8 weeks. **A** and **D,** Body weight of *Ptgs1*$^{-/-}$ mice (**A**) and *Ptgs2*$^{-/-}$ mice (**D**) as compared to respective wild-type (WT) littermates before (time 0) and at the indicated number of weeks after surgery. There was no significant difference between the genotypes. **B** and **E,** Safranin O staining of the medial portion of tibial cartilage 8 weeks after surgery in *Ptgs1*$^{-/-}$ mice (**B**) and 8 and 12 weeks after surgery in *Ptgs2*$^{-/-}$ mice (**E**), as compared to WT littermates. Representative samples are shown. Bars = 20 μm. **C** and **F,** Quantification of OA development in *Ptgs1*$^{-/-}$ mice (**C**) and *Ptgs2*$^{-/-}$ mice (**F**) as compared to WT littermates, by our grading system. There was no significant difference between the genotypes. Results obtained using the Osteoarthritis Research Society grading system were the same (data not shown). Values in **A, C, D,** and **F** are the mean ± SD of 5 mice per group.

Ptgs2$^{-/-}$ mice (Figure 3). The body weight of the 2 knockout mouse strains did not differ significantly from that of respective wild-type littermates before or after surgery ($P > 0.05$) (Figures 3A and D). Furthermore, OA development as assessed by cartilage degradation and osteophyte formation was not altered by the genetic deficiency of either *Ptgs1* or *Ptgs2* (Figures 3B, C, E, and F). The expression of other PGE_2 synthetic enzymes was not altered in the *Ptgs1*$^{-/-}$ or *Ptgs2*$^{-/-}$ mouse cartilage (data available from the corresponding author upon request), indicating a lack of compensatory regulation among the enzymes.

DISCUSSION

The present study showed that COX-2 was increased, while COX-1 was decreased, in joint cartilage during OA development. Further experiments using the inhibitor and genetic deficiency, however, demonstrated a lack of functional involvement of the 2 COX enzymes in OA development, at least in this experimental model. Contrary to expectations, COX-2 suppression did not ameliorate cartilage degradation, nor did COX-1 suppression exacerbate it. In a previous study using the same model, we similarly found that OA development was not prevented in mPGES-1–knockout mice (14). Besides these PG synthetic enzymes, proinflammatory cytokines, e.g., IL-1, TNFα, and IL-6, are believed to play significant roles in OA development. However, we previously showed that levels of these cytokines in synovial fluid from the knee joints of OA patients were much lower than those in rheumatoid arthritis patients (15). Furthermore, in a preliminary examination of *Il1a*$^{-/-}$;*Il1b*$^{-/-}$ and *Tnfa*$^{-/-}$ mice with experimental OA, we found that neither deficiency led to protection against cartilage degradation or osteophyte formation, although such protection occurred in *Cebpb*$^{+/-}$ mice studied as a positive control, as we reported previously (16) (data available from the corresponding author upon request).

Hence, inflammation might not have a major role in the pathogenesis of OA, although it may be secondary to cartilage degradation as a consequence of OA. It has been reported that the endochondral ossification process that is essential for fracture healing, rather than inflammation, plays an important role in OA development (9). Interestingly, however, both *Ptgs2*$^{-/-}$ and *Ptges*$^{-/-}$ mice showed normal OA development but impaired fracture healing (14,17). The reason for this discrepancy may be that OA development, including osteophyte formation, might be less dependent on in-